PUBLISHER :

Address of Publisher & Editor's Office :

GDAŃSK UNIVERSITY
OF TECHNOLOGY
Faculty
of Ocean Engineering
& Ship Technology

ul. Narutowicza 11/12
80-952 Gdańsk, POLAND
tel.: +48 58 347 17 93
fax : +48 58 341 47 12
e-mail : sekoce@pg.gda.pl

Account number :
BANK ZACHODNI WBK S.A.
I Oddział w Gdańsku
41 1090 1098 0000 0000 0901 5569

Editorial Staff :
Witold Kirkor Editor in Chief
e-mail : kirwik@interia.pl
Przemysław Wierzchowski Scientific Editor
e-mail : wierzche@xl.wp.pl
Maciej Pawłowski Editor for review matters
e-mail : mpawlow@pg.gda.pl
Tadeusz Borzęcki Editor for international relations
e-mail : tadbor@pg.gda.pl
Cezary Spigarski Computer Design
e-mail : cezarys@box43.pl

Domestic price :
single issue : 20 zł

Prices for abroad :
single issue :
- in Europe US$ 15
- overseas US$ 20

ISSN 1233-2585

POLISH MARITIME RESEARCH

in internet

www.bg.pg.gda.pl/pmr.html

Index and abstracts of the papers 1994 ÷ 2003

POLISH MARITIME RESEARCH

No 2(40) 2004 Vol 11

CONTENTS

The papers published in this issue have been reviewed by :
Prof. J. Girtler, Prof. J. Lisowski, Prof. K. Rosochowicz, Prof. K. Wierzcholski, M. Sperski, Assoc. Prof.

Editorial

POLISH MARITIME RESEARCH is a scientific journal of worldwide circulation. The journal appears as a quarterly four times a year. The first issue of it was published in September 1994. Its main aim is to present original, innovative scientific ideas and Research & Development achievements in the field of :

Engineering, **Computing & Technology**, **Mechanical Engineering**,

which could find applications in the broad domain of maritime economy. Hence there are published papers which concern methods of the designing, manufacturing and operating processes of such technical objects and devices as : ships, port equipment, ocean engineering units, underwater vehicles and equipment as well as harbour facilities, with accounting for marine environment protection.
The Editors of POLISH MARITIME RESEARCH make also efforts to present problems dealing with education of engineers and scientific and teaching personnel. As a rule, the basic papers are supplemented by information on conferences , important scientific events as well as cooperation in carrying out international scientific research projects.

Editorial Board

Research on deformations of laser-welded joint of a steel sandwich structure model

Dariusz Boroński
Academy of Agriculture & Engineering, Bydgoszcz
Janusz Kozak
Gdańsk University of Technology

ABSTRACT

Problems of the behaviour of all-steel, laser welded sandwich panels in plate-to-web contact zone are presented. Results of laboratory tests on determination of deformation field around laser weld under bending load – obtained by laser interferometry technique – are shown. Analysis of strain field distribution is included and some conclusions related to modeling of behaviour of such connection are drawn.

Key words : laser welding, laboratory tests of structural elements, laser interferometry

INTRODUCTION

Developments in novel joining techniques including laser, hybrid (laser – MAG) and friction stir welding have brought about their broader and broader industrial applications, as well as they opened new possibilities for designers to create structures not feasible so far.

Higher accuracy of so made welds and their more uniform quality, increased speed of welding, reduced amount of heat introduced to weld zone, possible automation and use of robots for welding processes – these are some advantages deciding upon fast application of such techniques in space, aircraft, car or shipbuilding industries [1, 2, 3, 4, 5, 6].

Their special position in the case of the application e.g. in shipbuilding [7] or aircraft industry is associated with, a.o., the possibility of building the sandwich structures which consist of load-carrying shell platings stiffened by cores of various forms, that leads, a.o., to a significant reduction of mass of designed objects. However application of the novel solutions usually demands some changes to be introduced to the traditional methods of construction of such objects as aircrafts and ships.

One of the example solutions based on the laser welding technique is a steel double-skin structure stiffened by internal webs joined with the shell platings by using laser welding applied from outside of the object under construction.

The idea of the replacement of the traditional single-skin ship hull structure with a new thin double-skin structure whose system of basic stiffening members is installed in the space between the shell platings, was born in the 1950s, and then it was studied by NASA [8, 9, 10]; however its practical application was attempted by US Navy at the end of the 1980s [11]. Presently Meyer Werft, Germany, applied the solution to the structural panels which appeared ten times stiffer and weighing less by 35% than their conventional equivalents [12].

Such panels have been produced and applied on an industrial scale e.g. to decks of Danube navigation passenger ships built in series by a German shipyard, as well as to bulkhead structures of another passenger ship [13].

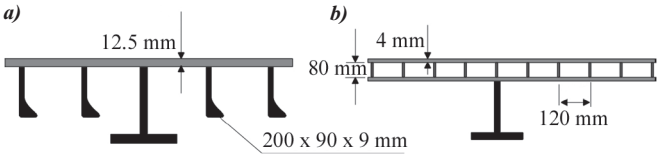

Fig.1. *Comparison of a classical deck structure* ***(a)*** *of a ro-ro ship and that built of Meyer's laser-welded panels* ***(b)***

However in order to apply the novel structural elements on a large scale – especially to important elements of ship hull structure – it is necessary to have at one's disposal information about their corrosion and fire resistance, and first of all about their technological and strength properties required to obtain approval of ship classification institutions.

The problems have become the theme of the „Sandwich" research program being realized in the scope of 5th Frame Program financially supported by European Commission. Within the research program a team of the Faculty of Ocean Engineering and Ship Technology, Gdańsk University of Technology, carried out verification of strength properties of full-scale double-skin panels internally stiffened by real stiffening member systems and different types of fillers [14]. Some new research problems which have resulted from the above mentioned work, are presently continued in the frame of the ASPIS project realized by the Faculty within EUREKA E!3074 program.

The steel double-skin panels differ from their classical single-skin counterparts by their shear stiffness in the direction of the stiffeners (webs), much greater than that in the direction perpendicular to them, i.e. Dqx>>Dqy. Simultaneously the stiffness is much smaller than that of the relevant classical struc-

ture. It means that apart from the collapse mechanisms which may occur in one of the stiffened platings, similar to those possible to occur in the traditional single-skin structures, other mechanisms resulting from mutual interaction of both platings may additionally occur, e.g. a kind of „rotation" of the elements relative to each other around the laser weld as a „hinge" (Fig.2).

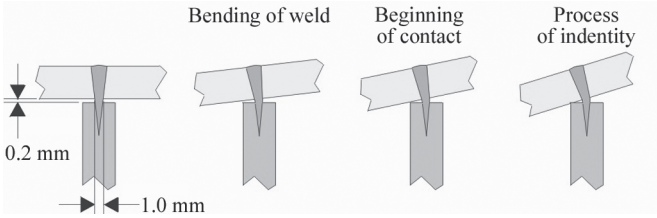

Fig. 2. *Behaviour of laser-welded joint under transverse load*

The phenomenon may be very important for the modelling of behaviour of a structure by means of the finite element method (FEM). By neglecting it an excessively high stiffness characteristics of a modeled structure against that real, may be erroneously calculated. Therefore from the point of view of modelling the behaviour of the entire panel under load it is important to know the macro-scale response of the joint.

The laser-welded joint much differs from a conventional arc-welded joint. As a result of the laser welding a narrow weld surrounded by a small heat-affected zone but with entirely different material properties against those of native material, is obtained.

No universal guidelines (including fatigue test data) have been so far available for fatigue assessment of laser welds, as this is the case for the traditionally made welds [15]. The available results of high-cycle fatigue tests of unnotched specimens containing laser weld [16] indicate that their fatigue strength does not much differ from that of the native material, which can partially result from the better quality (lack of defects) of the weld itself. The result can be also explained on the basis of the local strain approach to fatigue strength in the elastic range. However in the case of the load causing exceedance of the material yield point in the joint, strain values in particular weld zones will be different. It should be also taken into account that plastic strains may occurr not only due to large external loads but also as a result of a complex geometry of the joint leading to strain/stress concentration. Obviously all the above mentioned effects may occur in the considered steel sandwich panels.

In the reported work, being a part of the broader research program, the results of the first task of the research on local strain distribution in weld zone, due to the in-plane loading applied to the shell platings of the sandwich model structure, are presented. In the next phase of the investigations it is intended to analyze strains developed in weld zone during fatigue tests.

OBJECT AND METHOD OF THE RESEARCH

The research program was aimed at revealing the local phenomena in the laser-welded joint under bending in order to collect information necessary for modelling the joint's behaviour. The object (specimen) used in the research represented a fragment of a steel sandwich panel. In Fig.3 its structural arrangement and basic dimensions are shown. In its measurement part the specimen contained three webs joined with both shell platings. The investigations were focused on the joint connecting the middle web with one of the shell platings. The specimens were made of hull structural steel of known mechanical properties.

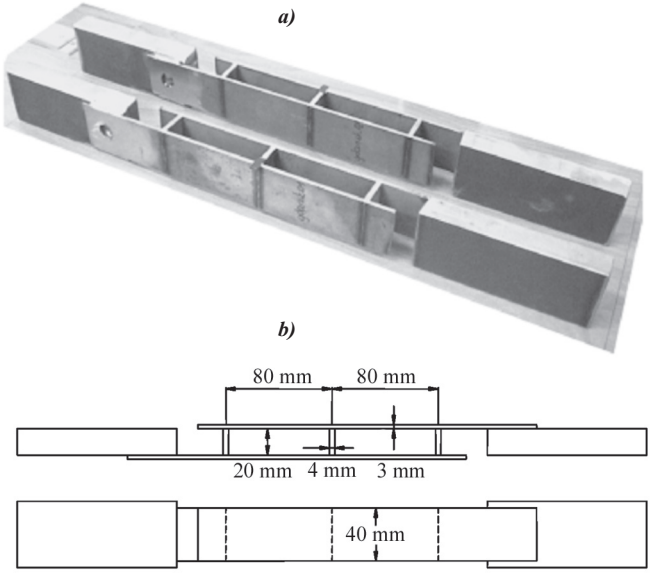

Fig. 3. *The structural arrangement* ***(a)*** *and the main dimensions* ***(b)*** *of the specimens*

The laser grating interferometry technique [17, 18] applied in the automated laser grating extensometer LES [19, 20], was used to investigate strains in the joint and to account for local character of the phenomena occurring in a small area of the joint.

The technique is an optical full-field method based on the phenomenon of interference of two mutually coherent light beams projected on a measurement grating, which produce a pattern of interference lines (fringes) carrying information on relative displacements of the surface of a tested object. Sensitivity of the method depends on an applied laser wave-length and diffraction grating density. In the case of the LES it amounts to 0.42 μm per one interference line. Further analysis of the lines makes it possible to obtain the measurement sensitivity of the order of 20 nm.

The used research instrumentation consisted of the LES extensometer, a fatigue testing machine and PC- class computer together with its accompanying equipment, is shown in Fig. 4.

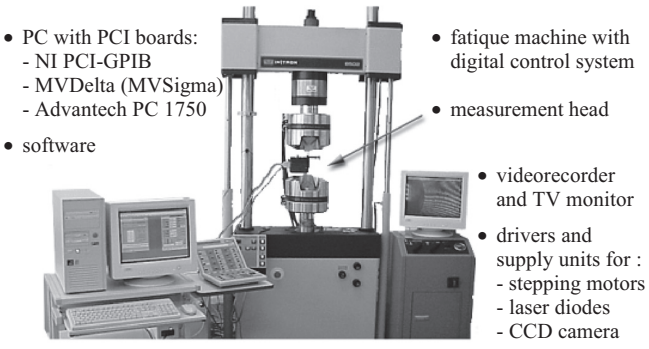

Fig. 4. *Configuration of the used research instrumentation*

Necessary calibration of the optical system can be remotely performed within the LES head. The pattern of interference lines (fringes) obtained during testing can be saved – through the electronic-optical vision system – in the computer memory. The pattern is partially analyzed in the real-time mode, which makes it possible to measure strains in a selected segment of measurement field, and the full information is saved on magnetic disk for further off-line analysis. Setting and operation

of the entire research instrumentation can be controlled by means of a special software.

The using of the laser interferometry method demands application of gratings placed onto the specimen's surface. In the investigations in question the gratings of the density of 1200 lines/mm obtained by dusting aluminium onto a matrix prepared on 2' x 2' glass plate, were used. During the preparation of the specimens for testing the 8 mm x 8 mm fragments of the grating were put on the cleaned surface of the joint by glueing the dusted aluminium layer, and then separating it from the matrix after setting the resin.

TEST RESULTS AND THEIR ANALYSIS

During the performed tests the distributions of relative displacements and strains in two mutually perpendicular directions U and V for 16 selected levels of static load (complying with Fig.6 and 8), were determined for values of the loading being under control. The tested specimen fitted with the LES head is shown in Fig.5. The specimens were loaded in accordance with the loading scheme shown in Fig.6.

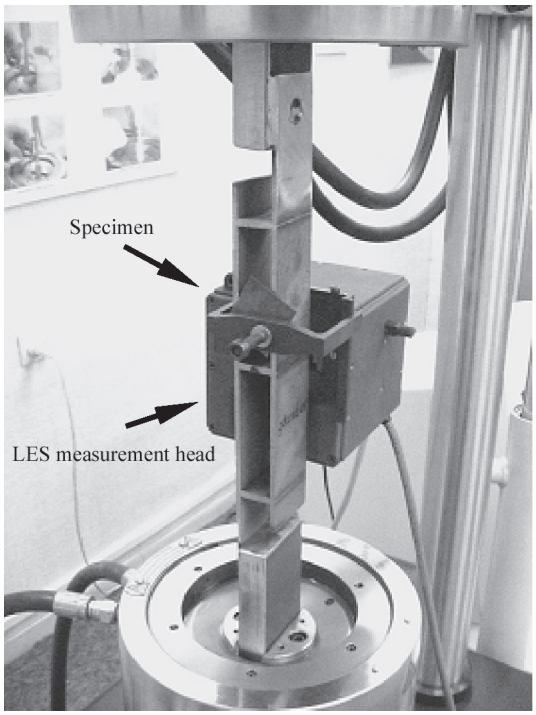

Fig. 5. *The sandwich structure model (specimen) under testing*

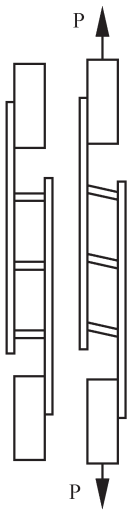

Loading levels

No	Load P [kN]
1.	0.00
2.	0.23
3.	0.55
4.	0.78
5.	0.98
6.	1.25
7.	1.54
8.	2.03
9.	2.28
10.	2.55
11.	2.77
12.	3.04
13.	3.27
14.	3.50
15.	3.82
16.	4.02
17.	0.00

Fig. 6. *Loading scheme of the specimen*

At particular values of the loading force P the fringe patterns in two analyzed directions U and V were recorded. The measurements were carried out for the middle joint only. The strain measurement field is shown in Fig.7.

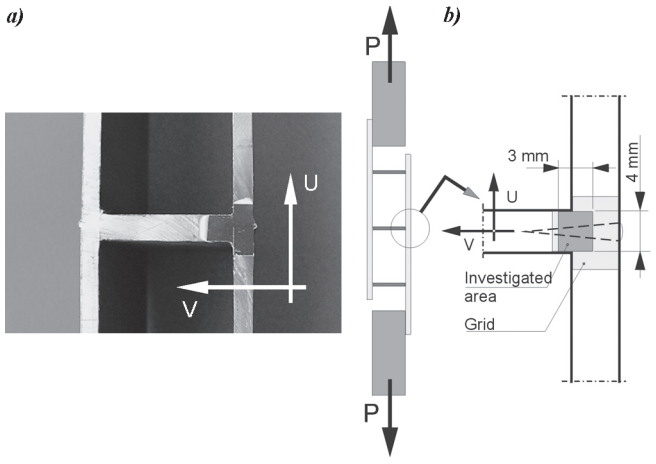

Fig. 7. *The specimen with the glued laser grating* ***(a)****, and the measurement field location relative to the laser weld* ***(b)***

The diagram of the load applied to a specimen in function of its elongation, together with the marked points of strain measurement, is presented in Fig.8. In the diagram the permanent elongation which remained in the specimen after unloading, is additionally indicated.

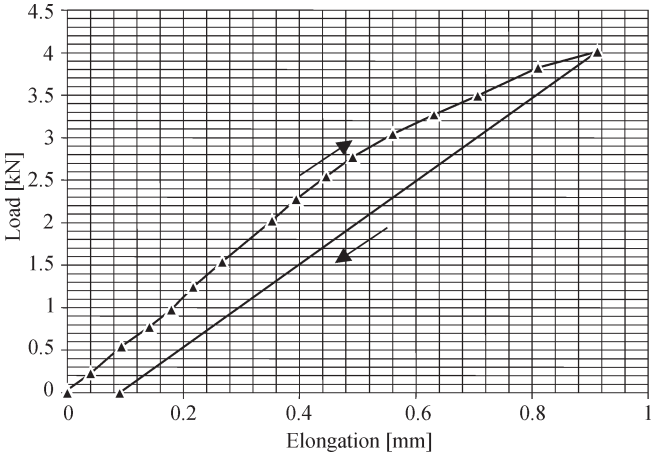

Fig.8. *The diagram of the load applied to a specimen in function of its elongation*

The example fringe patterns recorded during the tests are shown in Fig.9.

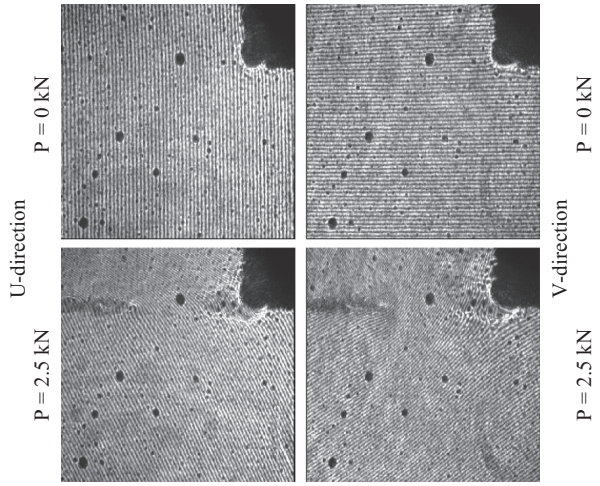

Fig.9. *The example fringe patterns recorded at P = 0 kN, and at P = 2.5 kN*

The strain analysis was generally limited to the values of the force P = 2.5 kN as large strain values occurred in the contact zone of the web and shell plate, which exceeded the basic measuring range of the applied method (for the mode of automatic measuring and data recording), as well as due to the concentration of fringes resulting from rotation of the specimen's elements under loading.

The obtained fringe patterns were analyzed with the use of numerical procedures making it possible to identify particular fringes and their phases within an analyzed field.

In Fig.10 and 11 are presented the strain distributions determined in the directions V and U, respectively, for successive values of the external force P.

The largest values of tensile strains (along V- axis) in the analyzed area occurred at the edge of the weld, and those of compressive strains – in the web-to-plate contact zone (Fig.12).

Along with increasing the load the increasing strain values occurred both in the compression and tension zones, also a gradual expansion of the zones into the plate material was observed.

The combined influence of the web bending and the web--to-plate contact on the strain distribution in the minimum cross--section of the weld, is shown in Fig.13.

From the analysis of the presented strain distribution it results that the neutral axis of bending, located close to the middle

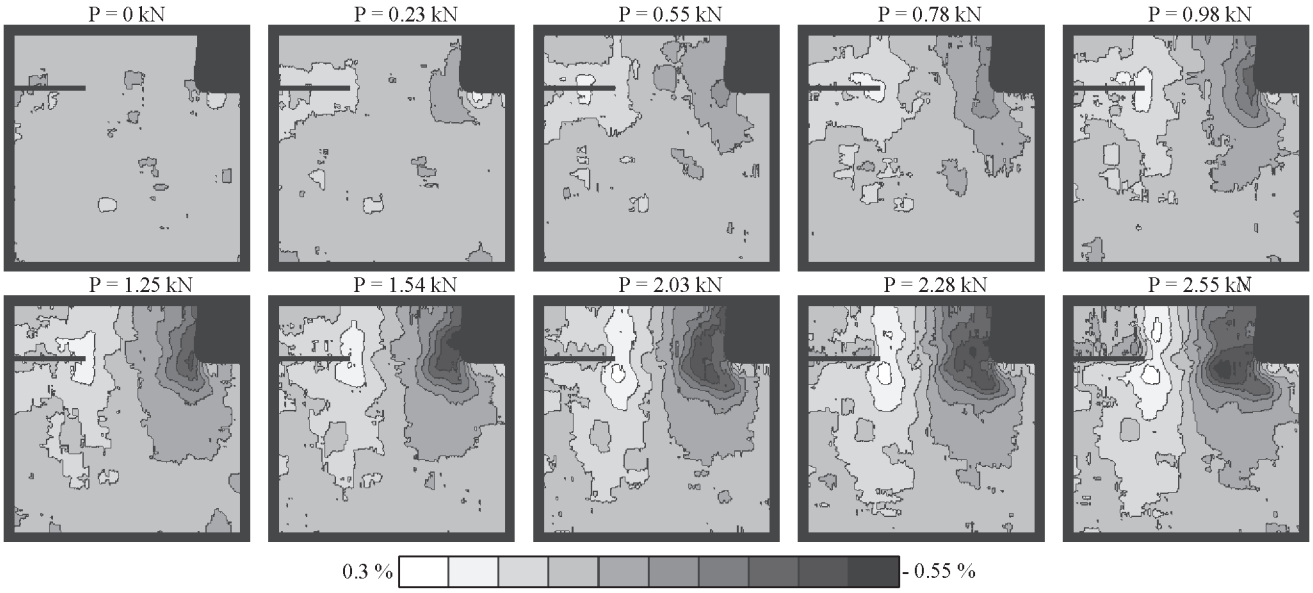

Fig.10. *Strain distributions in V-direction*

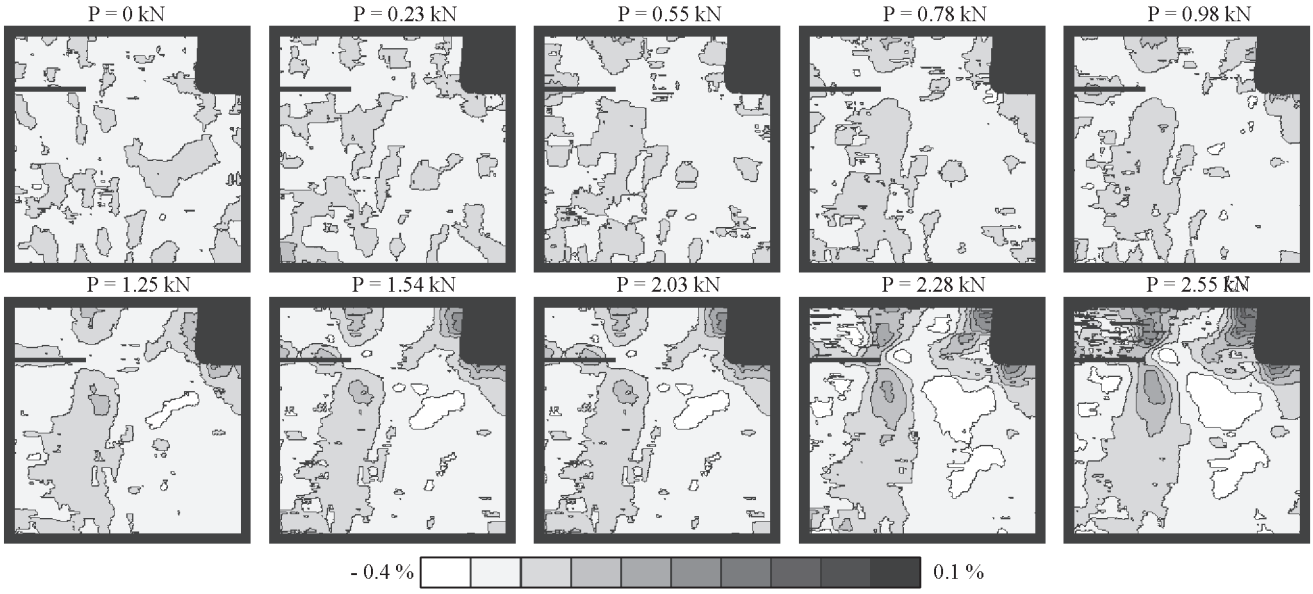

Fig.11. *Strain distributions in U-direction*

From the analysis of the obtained strain distributions along V-axis it can be observed that the axial load applied to the specimen in accordance with the loading scheme (Fig.8), generated a strain gradient typical for bending, in the surroundings of the weld joining the web with the shell plate.Simultaneously the edge of the web exerted contact pressure on the shell plate, that produced the compressive strain zones appearing both in the web and shell plate in the vicinity of the web's edge. (Fig.12).

of the weld, did not change its location despite the web came in contact with the plate during loading the specimen. As a result, only a deviation from linear distribution in the compressive strain zone of the weld occurred. Simultaneuously the contact pressure of the web on the shell plate caused large plastic strains in the contact zone, which exceeded the strains in the weld itself. Hence, such development of strains may indirectly indicate that the yield points of the weld, heat affected zone and native material could significantly differ from each other.

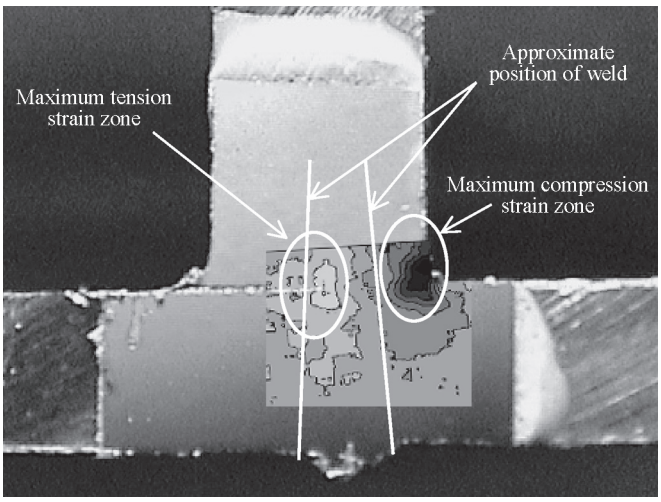

Fig.12. Strain distribution in the weld zone at P = 1.54 kN

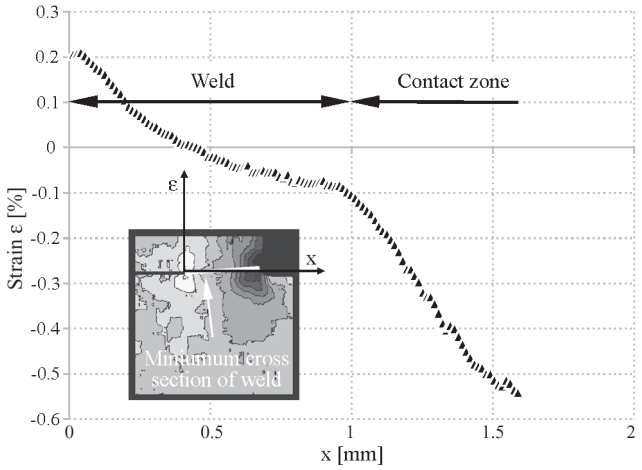

***Fig. 13.** The strain distribution in the minimum cross-section of the weld, at P = 1.54 kN*

Due to lack of a firm connection between the structural elements in the contact zone the plastic strains in the native material, resulting from compression remain unchanged, however the strains in the weld itself become smaller, that additionally increases the strain concentration effect in the heat affected zone during unloading the specimen.

The analysis of the strains in U-direction shows that they are symmetrically distributed with respect to the line running through the weld cross-section of the minimum area (Fig.14).

After detail analysis of the typical strain distribution shown in Fig.14.a, it was possible to suggest a probable character of the deformation of the joint containing laser weld, which is schematically shown in Fig.14.b. The web, while displacing relative to the shell plating, makes the laser weld formed of the material hardened due to welding process, rotating. The weld – while rotating – develops bending of the plate, manifested by two zones : of compressive and tensile strains, respectively, in the plate and web material on both sides of the weld. As a result, in the heat affected zone the strain gradients similar to those in the case of the strains in V-direction, appear.

CONCLUSIONS

- The investigation method applied in this work makes it possible to effectively determine strain distributions in the specimens of steel sandwich panels. The limitations associated with the exceedance of the basic measuring range of the method can be removed by using a sequential measurement procedure for the web and shell plate separately.
- The obtained strain distributions revealed much lower bending stiffness of the laser weld against the surrounding material, that made the entire joint more prone to deform. Due to a mutual „rotation" of the joined elements their edges (boundaries) come into mechanical contact in a short time.
- The contact phenomena revealed during the tests and the resulting asymmetrical behaviour of the joint imply to be very cautious in using the finite element method for modelling structural behaviour of the objects containing such joints. Application of the rutine approach and typical finite elements for structural analysis of such objects may lead to erroneous, and even unsafe results.
- In order to relate the observed effects associated with the developing of strain gradients to estimation of fatigue life of welded joints it would be necessary to perform a comprehensive fatigue test program covering, a.o., determination of weld-zone material properties under cyclic load and their changes during the testing. An analysis of the test results would make it possible to verify the present approach to the traditional welded joints. Knowing the local state of strains in the weld one would be able to apply the strain or energy approach to calculation of fatigue life of structures.

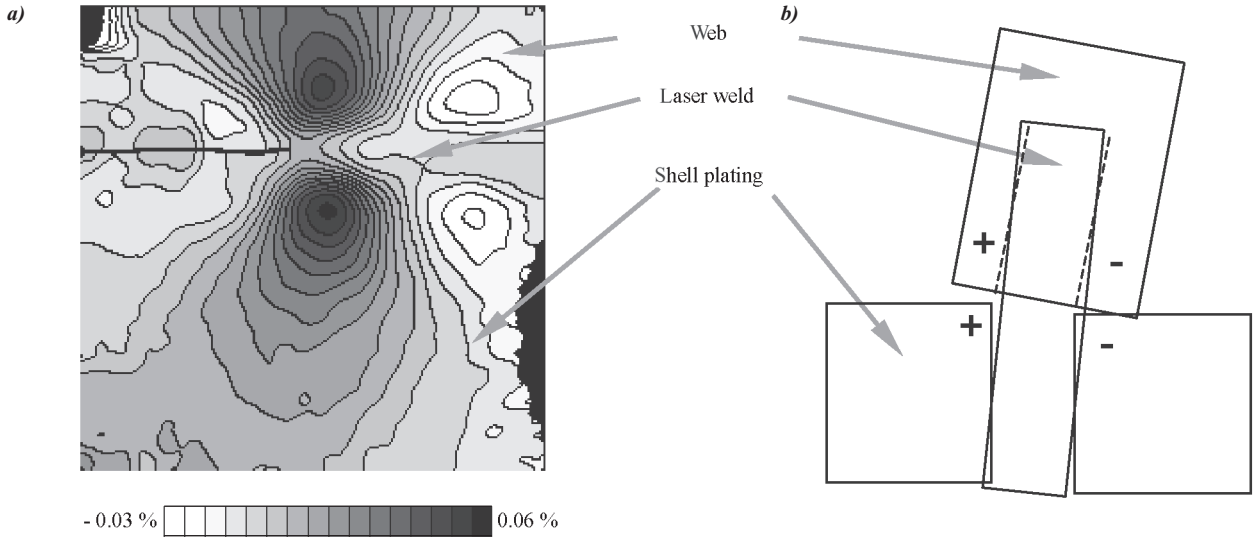

Fig.14.** Strain distribution in U-direction **(a)**, and scheme of deformation of the joint **(b)

ACRONIMS

ASPIS - Application of Steel Panels into Ship Structure
EMAS - Publisher
FEM - Finite element method
FPSOs - Floating Production, Storage and Offloading Units
IIW - International Institute of Welding
IRCN - Institut de Recherches de la Construction Navale
LES - Laser Grid Extensometer
MAG - Metal - Active - Gas
NASA - National Aeronautics & Space Agency
RINA - Royal Intitution of Naval Architects
SEM - Society for Experimental Mechanics
TWI - The Welding Institute
VTT - Valtion Teknillinen Tutkimuskeskus

BIBLOGRAPHY

1. Williams J. C., Starke Jr E. A.: *Progress in structural materials for aerospace systems*. Acta Materialia 51, 2003
2. Denney P. E., Fallara P. M., Brown L. E., Carney J. U., Woods G. D.: *Hybrid Laser Weld Development for Shipbuilding Applications*. The Society of Naval Architects and Marine Engineers, 2002 Annual Meeting – Ship Production Symposium and Expo, 25-27 September 2002, Boston, USA
3. Vilpas M., Kyröläinen A.: *Novel stainless steel solutions in bus structures*. VTT. Industrial Systems Review 2002
4. Kallee S. W., Nicholas E. D., Thomas W. M.: *Friction stir welding - invention, innovations and applications*. INALCO 2001 – 8th International Conference on Joints in Aluminium. Műnich, Germany, 28-30 March 2001
5. Thomas W. M., Woollin P., Johnson K. I.: *Friction stir welding of steel; A Feasibility Study.* Steel World, Vol. 4, No 2, 1999
6. Verhaeghe G.: *Laser welding automotive steel and aluminium*. „Make it With LASERS™ Workshop". Meeting on „Lasers in the automotive and sheet metal industries". TWI. Great Abington, UK, 13 July 2000
7. Roland F., Lambeck H.: *Laser beam welding in shipbuilding*. Proceedings of 7th International Aachen Welding Conference, High Productivity Joining Processes. Aachen, Germany, May 2002
8. Tat-Ching Fung : *Shear Stiffness for C-core Sandwich Panels*. Journal of Structural Engineering. August 1996
9. T. S. Lok, Q. H. Cheng : *Elastic Stiffness Properties and Behaviour of Truss-core Sandwich Panels*. Journal of Structural Engineering. May 2000
10. T. S. Lok, Q. H. Cheng : *Elastic Deflection of Thin-Walled Sandwich Panel*. Journal of Sandwich Structures and Materials, October 1999
11. Tanguy Quesnel : *Preliminary Study on Steel Composite Sandwich Panels : Shipbuilding Application*. IRCN papers. Nantes, France
12. Dolby R. E.: *Trends in welding processes in engineering construction for infrastructure projects.* 56th IIW Annual Assembly. Bucharest, Romania, 6 - 11 July 2003
13. Directory of Meyer Werft – Jos. L. Meyer GmbH. Papenburg, Germany (www.i-core.com)
14. Kozak J.: *Fatigue Properties of Laser Welded Steel Sandwich Panels.* Proceedings of Advanced Marine & Technology Application Conference. RINA. London, 9-10 October 2003
15. Maddox S. J.: *Fatigue design rules for welded structures*. Progress in Structural Engineering and Materials, Vol. 2, No 1, January – March 2000
16. Maddox S. J.: *Recommended Hot-Spot Stress Design S-N Curves for Fatigue Assessment of FPSOs*. International Journal of Offshore and Polar Engineering (Paper also given at ISOPE 2001 - 10th International Offshore and Polar Engineering Conference. Stavanger, Norway, 17-22 June 2001)
17. Post D.: *Developments in moiré interferometry.* Optical Engineering, Vol. 21, No 3/1982
18. Post D.: *Moiré interferometry* Handbook on Experimental Mechanics. Edited by A. Kobayashi. SEM, 1993
19. Boroński D., Giesko T., Sałbut L.: *The design and realisation of the laser grating interferometer for full field strain analysis in structural parts* (in Polish), Proceedings of 20th Symposium on Fundamentals of Machine Design. Scientific bulletin Mechanika, No 270. Opole, 2001
20. Boroński D., Szala J.: *Laser grating extensometer LES for fatigue full-field strain analysis.* European Conference on Fracture 14 - Fracture Mechanics Beyond 2000. EMAS. 2002

CONTACT WITH THE AUTHORS

Dariusz Boroński, D.Sc.
Mechanical Faculty
Academy of Agriculture & Engineering
85-796 Bydgoszcz, POLAND
Kaliskiego 7
e-mail : daborpkm@atr.bydgoszcz.pl

Janusz Kozak, D.Sc.
Faculty of Ocean Engineering
and Ship Technology
Gdańsk University of Technology
Narutowicza 11/12
80-952 Gdańsk, POLAND
e-mail : kozak@pg.gda.pl

FOREIGN *conference*

Maritime Transport 2003

On 25÷28 November 2003 in Barcelona
2nd International Conference on :

Maritime Transport & Maritime History

organized by Department of Nautical Science and Engineering, Technical University of Catalonia, and Maritime Museum in Barcelona, had place.

During the Conference 72 papers were presented.

Most of the papers (14 and 9) concerned maritime transport and environmental protection, whereas 5 presentations reminding maritime history which allows understanding ways of development and contemporary state of the art of the maritime knowledge and activities, deserved special attention. The presentation was enriched by visiting the Maritime Museum.

Two sessions were carried out in Tarragona where the Conference participants had the occasion to visit the local Mediterranean port tightly connected with the important Spanish petrochemical complex and industrial centre.

Prof. W. Galor of Maritime University of Szczecin (Poland) took part in the activity of International Scientific Committee of the Conference; he also chaired one of the sessions on "Simulators and control systems" and presented - during the session on "Training and simulations" - the paper on : "*The navigational analysis of modernization of Łeba port entrance*".

Moreover, during the session on "Ship development and hydrodynamics" dr. Józef Kozak, Gdańsk University of Technology (Poland), read the paper on : "*Strength tests of steel sandwich panels*".

Viscoelastic unsteady lubrication of radial slide journal bearing at impulsive motion

Andrzej Miszczak
Gdynia Maritime University

ABSTRACT

This paper presents an analytical solution of velocity components of unsymmetrical oil flow and pressure distribution in radial journal bearing gap for hydrodynamic unsteady lubrication with viscoelastic oil. Numerical calculations are performed in Mathcad 11 Professional Program, with taking into account the method of finite differences. This method satisfies stability conditions of numerical solutions of partial differential equations and values of capacity forces occurring in cylindrical bearings. Exact calculations of pressure in journal bearing and its load capacity may be useful to prevent from premature wear tribological units of self ignition engines, especially those applied in ships.

Key words : viscoelastic unsteady lubrication, analytical and numerical calculation, capacity forces, hydrodynamic pressure

INTRODUCTION

Correctness assessment of functioning the machines used for driving systems of various transport means e.g. diesel engines in which journal friction units are installed, depends to a large extent on assumed computational models, correct estimation of assumed appropriate simplifications, if necessary, and then on an assumed numerical method for the determining of operational parameters. During maneouvres of sea-going ships as well as when driving cars many frequent changes of engine operational parameters occur, especially of its rotational speed and loading. Similarly it happens during sailing the ship in rough weather when non-stationary loads on its propulsion engine happen.

Both car vehicles and majority of sea-going ships are equipped with a propulsion system of a single self-ignition combustion engine. Seizure of trigological system of such engine is equivalent to depriving the vehicle or ship of its propulsion and thereby of its serviceability [3]. If such an event occurs during storm emergency situations or even a catastrophy may happen [4]. One of the ways to avoid such failures is to apply a lubricating oil of required properties, especially of appropriate viscosity and lubricity.

Therefore the main aim of this work is to present analytical-numerical calculations of distributions of hydrodynamic pressure values occurring during non-stationary impulse lubrication of bearing surfaces at viscoelastic oil flow. Viscoelastic properties are characteristic for all oils which contain various bettering admixtures or in which some impurities such as lead salts, soot or dust, happen. All such impurities and admixtures are typical for land and sea transport.

Taking into account the above mentioned observations it is necessary to precisely analyze the influence of non-stationary load impulses which are transferred through a propulsion system to a slide friction unit and result in such characteristic quantity of the bearing as its load-carrying capacity determined on the basis of pressure distributions.

In Fig.1 the structure and loading scheme of a slide journal bearing is presented.

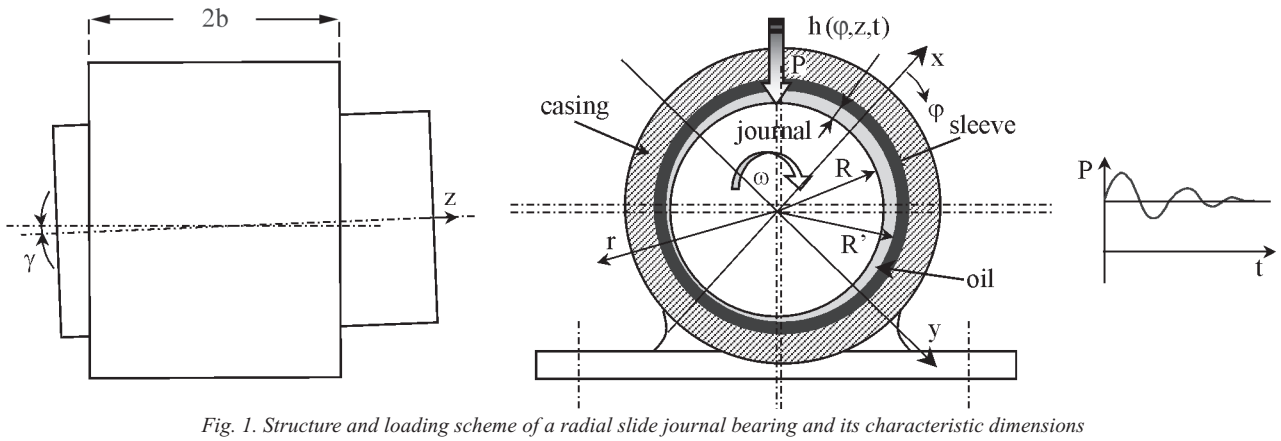

Fig. 1. Structure and loading scheme of a radial slide journal bearing and its characteristic dimensions

As shown in the scheme the bearing sleeve axis may undergo a skew respective to the journal axis. The quantity is described by the angle γ. In such case the oil gap height depends on the tangential variable φ and the longitudinal coordinate z. In the case of non-stationary impulse loads the oil gap height additionally depends on time t.

THEORETICAL MODEL

Oil flow through the cylindrical gap height of radial slide bearing is described by the momentum conservation equations and continuity equation [1, 2, 6, 7, 8, 10, 11, 15]. Additionally, Rivlin-Ericksen constitutive relationships were assumed. The equations in question are of the following form :

$$\mathrm{Div}\,\mathbf{S} = \rho d\mathbf{v}/dt \quad , \quad \mathrm{div}\,\mathbf{v} = 0 \quad , \quad \mathbf{S} = -p\mathbf{I} + \eta_o\mathbf{A}_1 + \alpha(\mathbf{A}_1)^2 + \beta\mathbf{A}_2 \tag{1}$$

where :

S	- stress tensor	ρ	- oil density
Div **S**	- stress tensor divergence	t	- time
v	- velocity vector	p	- pressure
div **v**	- velocity vector divergence	**I**	- unit tensor

$\mathbf{A}_1$ and $\mathbf{A}_2$ - two Rivlin-Ericksen strain tensors of three material constants η_o, α, β,

where :

η_o - dynamic viscosity α, β - pseudo-viscosity constans of oil

The coordinates of $\mathbf{A}_1$, $\mathbf{A}_2$ tensors are described by the symmetrical matrices defined as follows :

$$\begin{gathered}\mathbf{A}_1 \equiv \mathbf{L} + \mathbf{L}^T \\ \mathbf{A}_2 \equiv \mathrm{grad}\,\mathbf{a} + (\mathrm{grad}\,\mathbf{a})^T + 2\mathbf{L}^T\mathbf{L} \\ \mathbf{a} \equiv \mathbf{L}\mathbf{v} + \frac{\partial \mathbf{v}}{\partial t}\end{gathered} \tag{2}$$

where :

L	- tensor of oil velocity vector gradient s^{-1}	**a**	- acceleration vector
$\mathbf{L}^T$	- tensor with matrix transpose s^{-1}	grad **a**	- acceleration vector gradient

The product of the Deborah and Strouhal numbers, marked DeStr, is assumedof the same order as the product of the Reynold's number, relative radial clearance and Strouhal number, marked ReψStr. Moreover : $\mathrm{DeStr} >> \mathrm{De} \equiv \alpha\omega/\eta_o$.
where : ψ - relative radial clearence, and ω - angular speed of cylindrical bearing journal.

The following is additionally assumed :

- rotational motion of the journal with the tangential speed $U = \omega R$
- unsymmetrical, non-stationary oil flow through bearing gap height
- non-stationary viscoelastic properties of oil
- constant oil density ρ
- the characteristic gap height $h(\varphi,z,t)$, in the cylindrical bearing
- no slip between bearing surfaces
- R - radius of cylindrical journal
- 2b - length of the bearing in question.

Neglecting the terms for the relative radial clearance $\psi \equiv \varepsilon/R \cong 10^{-3}$ in the basic equations defined in the cylindrical coordinate frame : φ, r, z, as well as taking into account the above mentioned assumptions, one can obtain :

$$\frac{\partial v_\varphi}{\partial t} = -\frac{1}{\rho R}\frac{\partial p}{\partial \varphi} + \frac{\eta_o}{\rho}\frac{\partial}{\partial r}\left(\frac{\partial v_\varphi}{\partial r}\right) + \frac{\beta}{\rho}\frac{\partial^3 v_\varphi}{\partial t \partial r^2} \tag{3}$$

$$0 = \frac{\partial p}{\partial r} \tag{4}$$

$$\frac{\partial v_z}{\partial t} = -\frac{1}{\rho}\frac{\partial p}{\partial z} + \frac{\eta_o}{\rho}\frac{\partial}{\partial r}\left(\frac{\partial v_z}{\partial r}\right) + \frac{\beta}{\rho}\frac{\partial^3 v_z}{\partial t \partial r^2} \tag{5}$$

$$\frac{1}{R}\frac{\partial v_\varphi}{\partial \varphi} + \frac{\partial v_r}{\partial r} + \frac{\partial v_z}{\partial z} = 0 \tag{6}$$

for : $0 \le \varphi < 2\pi$, $-b \le z \le +b$, $0 \le r \le h$, where : h - characteristic gap height.

The symbols: v_φ, v_r, v_z represent the respective oil velocity vector components : tangentially directed, that along gap height, and longitudinally directed. The following relationships between the dimensional and dimensionless quantities are assumed [12 , 13] :

$$\begin{gathered}r = R(1+\psi r_1) \ , \ z = bz_1 \ , \ t = t_o t_1 \ , \ h = \varepsilon h_1 \ , \ v_\varphi = U v_{\varphi 1} \ , \ v_r \equiv U\psi\, v_{r1} \\ v_z \equiv (U/L_1)\, v_{z1} \ , \ p = p_o p_1 \ , \ p_o \equiv U\eta_o R/\varepsilon^2 \ , \ L_1 = b/R\end{gathered} \tag{7}$$

Reynolds number, modified Reynolds number, Strouhal and Deborah number are assumed in the following forms :

$$\mathrm{Re} \equiv \rho U \varepsilon / \eta_o \ , \ \mathrm{Re}\psi \equiv \rho \omega \varepsilon^2 / \eta_o \ , \ \mathrm{Str} \equiv R/(Ut_o) \ , \ \mathrm{De} \equiv \beta U/(\eta_o R) \tag{8}$$

hence :

$$\mathrm{DeStr} = \beta/(\eta_o t_o) \equiv \mathrm{Des} \ , \ \mathrm{Re}\psi\mathrm{Str} = \rho\varepsilon^2/(\eta_o t_o) \equiv \mathrm{Res} \tag{8a}$$

For the commonly applied inhibitors the coefficient β satisfies the inequality: $0 < \beta/t_o < \eta_o$. Values of the coefficient β vary from 0.000001 Pa·s^2 to 0.01 Pa·s^2. The dimensionless symbols are marked with the lower index "1". The equations (3) ÷ (6) take the dimensionless form :

$$\mathrm{Res}\frac{\partial v_{\varphi 1}}{\partial t_1} = -\frac{\partial p_1}{\partial \varphi} + \frac{\partial}{\partial r_1}\left(\frac{\partial v_{\varphi 1}}{\partial r_1}\right) + \mathrm{Des}\frac{\partial^3 v_{\varphi 1}}{\partial t_1 \partial r_1^2} \tag{9}$$

$$0 = \frac{\partial p_1}{\partial r_1} \tag{10}$$

$$\mathrm{Res}\frac{\partial v_{z1}}{\partial t_1} = -\frac{\partial p_1}{\partial z_1} + \frac{\partial}{\partial r_1}\left(\frac{\partial v_{z1}}{\partial r_1}\right) + \mathrm{Des}\frac{\partial^3 v_{z1}}{\partial t_1 \partial r_1^2} \tag{11}$$

$$\frac{\partial v_{\varphi 1}}{\partial \varphi} + \frac{\partial v_{r1}}{\partial r_1} + \frac{1}{L_1^2}\frac{\partial v_{z1}}{\partial z_1} = 0 \tag{12}$$

for : $0 \le \varphi < 2\pi$, $-1 \le z_1 \le +1$, $0 \le r_1 \le h_1$

GENERAL AND PARTICULAR SOLUTIONS

A new variable is now introduced :

$$\chi \equiv r_1 N \ , \ N \equiv \frac{1}{2}\sqrt{\frac{\mathrm{Res}}{t_1}} \ , \ t_1 > 0 \ , \ 0 < \frac{\mathrm{Des}}{t_1} < 1 \tag{13}$$

and solutions are assumed to have the form of the following convergent series [5] :

$$v_{\varphi 1} = v_{\varphi 0\Sigma}(\chi,\varphi,z_1) + \frac{\mathrm{Des}}{t_1} v_{\varphi 1\Sigma}(\chi,\varphi,z_1) + \left(\frac{\mathrm{Des}}{t_1}\right)^2 v_{\varphi 2\Sigma}(\chi,\varphi,z_1) + ... \tag{14}$$

$$v_{z1} = v_{z0\Sigma}(\chi,\varphi,z_1) + \frac{\mathrm{Des}}{t_1} v_{z1\Sigma}(\chi,\varphi,z_1) + \left(\frac{\mathrm{Des}}{t_1}\right)^2 v_{z2\Sigma}(\chi,\varphi,z_1) + ... \tag{15}$$

$$v_{r1} = v_{r0\Sigma}(\chi,\varphi,z_1) + \frac{\mathrm{Des}}{t_1} v_{r1\Sigma}(\chi,\varphi,z_1) + \left(\frac{\mathrm{Des}}{t_1}\right)^2 v_{r2\Sigma}(\chi,\varphi,z_1) + ... \tag{16}$$

$$p_1 = p_{10}(\varphi,z_1,t_1) + \frac{\mathrm{Des}}{t_1} p_{11}(\varphi,z_1,t_1) + \left(\frac{\mathrm{Des}}{t_1}\right)^2 p_{12}(\varphi,z_1,t_1) + ... \tag{17}$$

for : $t_1 > 0$, $0 < \mathrm{Des} << 1$, $(\mathrm{Des}/t_1) < 1$

In the equations (9) ÷ (11) the derivatives respective to the variables t_1, r_1 are substituted for the derivatives relative to the variable χ, by using the relationships given in App. 1. Therefore the variables t_1, r_1 are substituted for the variable χ. Now the series (14) ÷ (17) are introduced to the equation system (9) ÷ (11). Next, the terms multiplied by the parameters of the same power, $(\mathrm{Des}/t_1)^k$, are successively compared for k = 0, 1, 2, ... Hence the following sequence of ordinary differential equations is obtained:

$$\frac{d^2 v_{\varphi 0\Sigma}}{d\chi^2} + 2\chi\frac{dv_{\varphi 0\Sigma}}{d\chi} = \frac{1}{N^2}\frac{\partial p_{10}}{\partial \varphi} \tag{18}$$

$$\frac{d^2 v_{z0\Sigma}}{d\chi^2} + 2\chi\frac{dv_{z0\Sigma}}{d\chi} = \frac{1}{N^2}\frac{\partial p_{10}}{\partial z_1} \tag{19}$$

$$\frac{d^2 v_{\varphi 1\Sigma}}{d\chi^2} + 2\chi\frac{dv_{\varphi 1\Sigma}}{d\chi} + 4v_{\varphi 1\Sigma} = \frac{1}{N^2}\frac{\partial p_{11}}{\partial\varphi} + \frac{d^2 v_{\varphi 0\Sigma}}{d\chi^2} + \frac{1}{2}\chi\frac{d^2 v_{\varphi 0\Sigma}}{d\chi^2} \tag{20}$$

$$\frac{d^2 v_{z1\Sigma}}{d\chi^2} + 2\chi\frac{dv_{z1\Sigma}}{d\chi} + 4v_{z1\Sigma} = \frac{1}{N^2}\frac{\partial p_{11}}{\partial z_1} + \frac{d^2 v_{z0\Sigma}}{d\chi^2} + \frac{1}{2}\chi\frac{d^2 v_{z0\Sigma}}{d\chi^2} \tag{21}$$

$$\frac{d^2 v_{\varphi 2\Sigma}}{d\chi^2} + 2\chi\frac{dv_{\varphi 2\Sigma}}{d\chi} + 8v_{\varphi 2\Sigma} = \frac{1}{N^2}\frac{\partial p_{12}}{\partial\varphi} + 2\frac{d^2 v_{\varphi 1\Sigma}}{d\chi^2} + \frac{1}{2}\chi\frac{d^3 v_{\varphi 1\Sigma}}{d\chi^3} \tag{22}$$

$$\frac{d^2 v_{z2\Sigma}}{d\chi^2} + 2\chi\frac{dv_{z2\Sigma}}{d\chi} + 8v_{z2\Sigma} = \frac{1}{N^2}\frac{\partial p_{12}}{\partial z_1} + 2\frac{d^2 v_{z1\Sigma}}{d\chi^2} + \frac{1}{2}\chi\frac{d^3 v_{z1\Sigma}}{d\chi^3} \tag{23}$$

and so on.

The general solutions of the differential equations (18), (19) are of the following form :

$$v_{\varphi 0\Sigma}(\chi,\varphi,z_1) = C_{\varphi 1}v_{01}(\chi) + C_{\varphi 2}v_{02}(\chi) + v_{\varphi 03}(\chi,\varphi,z_1) \tag{24}$$

$$v_{z0\Sigma}(\chi,\varphi,z_1) = C_{z1}v_{01}(\chi) + C_{z2}v_{02}(\chi) + v_{z03}(\chi,\varphi,z_1) \tag{25}$$

where: $C_{\varphi 1}$, $C_{\varphi 2}$, C_{z1} , C_{z2} are integration constants. The particular solutions of the uniform and non-uniform ordinary differential equation are as follows :

$$v_{01}(\chi) = \frac{\sqrt{\pi}}{2}\mathrm{erf}(\chi) \quad , \quad v_{02}(\chi) = 1 \quad , \quad \mathrm{erf}(\chi) \equiv \frac{2}{\sqrt{\pi}}\int_0^{\chi} e^{-\chi_1^2} d\chi_1 \tag{26}$$

$$v_{\varphi 03}(\chi,\varphi,z_1) = -\frac{\sqrt{\pi}}{2N^2}\frac{\partial p_{10}}{\partial\varphi}\Omega(\chi) \quad , \quad v_{z03}(\chi,\varphi,z_1) = -\frac{\sqrt{\pi}}{2N^2}\frac{\partial p_{10}}{\partial z_1}\Omega(\chi) \tag{27}$$

$$\Omega(\chi) \equiv \int_0^{\chi} e^{\chi_1^2}\mathrm{erf}\chi_1 d\chi_1 - \mathrm{erf}\chi\int_0^{\chi} e^{\chi_1^2} d\chi_1 \tag{28}$$

where : $0 \le \chi_1 \le \chi \equiv r_1 N$

For $t_1 \to 0$, one obtains $N \to \infty$, hence $\chi \to \infty$. If $t_1 \to \infty$, then $N \to 0$, as well as for $r_1 > 0$ one obtains $\chi \to 0$. If $t_1 > 0$ and $r_1 = 0$ then $\chi = 0$. The following limits are true :

$$\begin{aligned}
&v_{01}(\chi) = \pi^{0.5}/2 \quad \text{for : } \chi\to\infty \ , \ t_1\to 0 \ , \ N\to\infty \\
&v_{01}(\chi) = 0 \quad \text{for : } \chi\to 0 \ , \ r_1 = 0 \ , \ 0 < t_1 < t_2 < \infty \ , \ N > 0 \\
&v_{i03}(\chi) = 0 \quad \text{for : } \chi\to 0 \ , \ r_1 = 0 \ , \ 0 < t_1 < t_2 < \infty \ , \ N > 0 \ ; \ \text{where : } i = \varphi, z \\
&v_{01}(\chi) = 0 \quad \text{for : } \chi\to 0 \ , \ r_1 > 0 \ , \ t_1\to\infty \ , \ N\to 0
\end{aligned} \tag{29}$$

$$\begin{aligned}
v_{\varphi 03} &= -\frac{r_1^2}{2}\frac{\partial p_{10}}{\partial\varphi} \quad \text{for : } \chi\to 0 \ , \ r_1 > 0 \ , \ t_1\to\infty \ , \ N\to 0 \\
v_{z03} &= -\frac{r_1^2}{2}\frac{\partial p_{10}}{\partial z_1} \quad \text{for : } \chi\to 0 \ , \ r_1 > 0 \ , \ t_1\to\infty \ , \ N\to 0
\end{aligned} \tag{30}$$

The cylindrical journal executes only the rotational motion in the φ direction. Hence the oil velocity component on the journal surface in the tangential direction is equal to the velocity of the cylindrical surface of the journal.

The longitudinal component of oil velocity on the journal's cylindrical surface equals zero because the journal is motionless along the z-axis. However the shaft undergoes pulsatory changes of its location with time along the gap height direction. Hence the gap height is time dependent. Thus, the following boundary conditions appear :

$$\begin{gathered}
v_{\varphi 0\Sigma}(\chi = 0) = 1 \ , \ v_{z0\Sigma}(\chi = 0) = 0 \ , \ v_{r0\Sigma}(\chi = 0) = \mathrm{Str}\cdot(\partial h_1/\partial t_1) \\
\text{for : } r_1 = 0 \Leftrightarrow \chi = 0 \ , \ 0 < t_1 < t_2 < \infty \ , \ N > 0
\end{gathered} \tag{31}$$

The cylindrical sleeve surface is motionless in the tangential, longitudinal (axial) and radial directions. Viscous oil flows around the sleeve. Hence the oil velocity on the sleeve surface equals zero in the tangential and longitudinal directions as well as in the gap height direction r. Thus the following boundary conditions are valid :

$$\begin{gathered}
v_{\varphi 0\Sigma}(\chi = M) = 0 \ , \ v_{z0\Sigma}(\chi = M) = 0 \ , \ v_{r0\Sigma}(\chi = M) = 0 \\
\text{for : } r_1\to h_1 \Leftrightarrow \chi\to N h_1 \equiv M \ , \ 0 < t_1 < t_2 < \infty \ , \ N > 0 \\
\text{where : } h = \varepsilon h_1 \text{ - gap height} \ , \ h_1\text{- dimensionless gap height}
\end{gathered} \tag{32}$$

Applying the conditions (31), (32) to the solutions (24), (25) one obtains :

$$\begin{aligned}
&C_{\varphi 1}v_{01}(\chi = 0) + C_{\varphi 2} + v_{\varphi 03}(\chi = 0) = 1 \qquad \text{for : } r_1 = 0\\
&C_{\varphi 1}v_{01}(\chi = M) + C_{\varphi 2} + v_{\varphi 03}(\chi = M) = 0 \qquad \text{for : } r_1 = h_1\\
&C_{z1}v_{01}(\chi = 0) + C_{z2} + v_{z03}(\chi = 0) = 0 \qquad \text{for : } r_1 = 0\\
&C_{z1}v_{01}(\chi = M) + C_{z2} + v_{z03}(\chi = M) = 0 \qquad \text{for : } r_1 = h_1
\end{aligned} \tag{33}$$

If the limits (29), (30) are taken into account the set of equations (33) yields the following solutions :

$$C_{\varphi 1} = -\frac{1 + v_{\varphi 03}(M)}{v_{01}(M)} \;,\; C_{z1} = -\frac{v_{z03}(M)}{v_{01}} \;,\; C_{\varphi 2} = 1 \;,\; C_{z2} = 0 \tag{34}$$

Now, to the right hand sides of the equations (20), (21) the solutions (24), (25), (26), (27), (28), (34) are substituted. Hence the general solution of the equations (20), (21) obtains the following form :

$$v_{\varphi 1\Sigma}(\chi,\varphi,z_1) = C_{\varphi 3}v_{11}(\chi) + C_{\varphi 4}v_{12}(\chi) + v_{\varphi 13}(\chi,\varphi,z_1) \tag{35}$$

$$v_{z1\Sigma}(\chi,\varphi,z_1) = C_{z3}v_{11}(\chi) + C_{z4}v_{12}(\chi) + v_{z13}(\chi,\varphi,z_1) \tag{36}$$

where : $C_{\varphi 3}$, $C_{\varphi 4}$, C_{z3} , C_{z4} - integration constants

The particular solutions are as follows :

$$v_{11}(\chi) = \chi e^{-\chi^2} \tag{37}$$

$$v_{12}(\chi) = \chi e^{-\chi^2} \int_{\delta}^{\chi} \frac{1}{\chi_1^2} e^{-\chi_1^2} d\chi_1 \tag{38}$$

$$\begin{aligned}
v_{\varphi 13}(\chi,z_1,C_{\varphi 1}) &= v_{11}(\chi)\int_0^{\chi}\left\{C_{\varphi 1}\chi_1(\chi_1+2) - \left(1+\frac{\chi_1}{2}\right)e^{\chi_1^2}\frac{d^2}{d\chi_1^2}\left[v_{\varphi 03}(\chi_1)\right] + \frac{1}{N^2}\frac{\partial p_{11}}{\partial \varphi}\right\}v_{12}(\chi_1)d\chi_1 +\\
&+ v_{12}(\chi)\int_0^{\chi}\left\{\left(1+\frac{\chi_1}{2}\right)e^{\chi_1^2}\frac{d^2}{d\chi_1^2}\left[v_{\varphi 03}(\chi_1)\right] + \frac{1}{N^2}\frac{\partial p_{11}}{\partial \varphi} - C_{\varphi 1}\chi_1(\chi_1+2)\right\}v_{11}(\chi_1)d\chi_1\\
v_{z13}(\chi,z_1,C_{\varphi 1}) &= v_{11}(\chi)\int_0^{\chi}\left\{C_{z1}\chi_1(\chi_1+2) - \left(1+\frac{\chi_1}{2}\right)e^{\chi_1^2}\frac{d^2}{d\chi_1^2}\left[v_{z03}(\chi_1)\right] + \frac{1}{N^2}\frac{\partial p_{11}}{\partial z_1}\right\}v_{12}(\chi_1)d\chi_1 +\\
&+ v_{12}(\chi)\int_0^{\chi}\left\{\left(1+\frac{\chi_1}{2}\right)e^{\chi_1^2}\frac{d^2}{d\chi_1^2}\left[v_{z03}(\chi_1)\right] + \frac{1}{N^2}\frac{\partial p_{11}}{\partial z_1} - C_{z1}\chi_1(\chi_1+2)\right\}v_{11}(\chi_1)d\chi_1
\end{aligned} \tag{39}$$

for : $0 < \delta \le \chi_1 \le \chi$

The solutions (35), (36) represent corrections to the components of oil velocity because of its viscoelastic properties. On the basis of the solutions (37) ÷ (39) for $\chi \to 0$, $r_1 \to 0$, $N > 0$ the following limits are achieved :

$$\lim_{\chi\to 0, N>0} v_{12}(\chi) = \lim_{\chi\to 0, N>0} \chi e^{-\chi^2} \int_{\delta}^{\chi}\left(\frac{1}{\chi_1^2}\, e^{\chi_1^2}\right)d\chi_1 = -1 \tag{40}$$

The following limits are also true :

$$\begin{aligned}
&v_{11}(\chi) = 0 \quad \text{for : } \chi\to 0 \;,\; r_1 = 0 \;,\; 0 < t_1 < t_2 < \infty \;,\; N > 0\\
&v_{12}(\chi) = -1 \quad \text{for : } \chi\to 0 \;,\; r_1 = 0 \;,\; 0 < t_1 < t_2 < \infty \;,\; N > 0\\
&v_{i13}(\chi) = 0 \quad \text{for : } \chi\to 0 \;,\; r_1 = 0 \;,\; 0 < t_1 < t_2 < \infty \;,\; N > 0 \;;\; \text{where } i = \varphi, z
\end{aligned} \tag{41}$$

The corrections to the oil velocity components cannot have the same boundary conditions as those previously assumed (31), (32) for the cylindrical journal and sleeve in the longitudinal and tangential directions. Therefore the corrections satisfy the following boundary conditions :

$$\begin{aligned}
&v_{\varphi 1\Sigma}(\chi = 0) = 0 \;,\; v_{z1\Sigma}(\chi = 0) = 0 \quad \text{for : } r_1 = 0 \Leftrightarrow \chi = 0 \;,\; 0 < t_1 < t_2 < \infty \;,\; N > 0\\
&v_{\varphi 1\Sigma}(\chi = M) = 0 \;,\; v_{z1\Sigma}(\chi = M) = 0 \quad \text{for : } r_1 \to h_1 \Leftrightarrow \chi \to N h_1 \equiv M \;,\; 0 < t_1 < t_2 < \infty \;,\; N > 0
\end{aligned} \tag{42}$$

Applying the conditions (42) to the general solutions (35), (36) one obtains :

$$\begin{aligned} &C_{\varphi 3}v_{11}(\chi = 0) + C_{\varphi 4}v_{12}(\chi = 0) + v_{\varphi 13}(\chi = 0) = 0 \qquad \text{for : } r_1 = 0 \\ &C_{\varphi 3}v_{11}(\chi = M) + C_{\varphi 4}v_{12}(\chi = M) + v_{\varphi 13}(\chi = M) = 0 \qquad \text{for : } r_1 = h_1 \\ &C_{z3}v_{11}(\chi = 0) + C_{z4}v_{12}(\chi = 0) + v_{z13}(\chi = 0) = 0 \qquad \text{for : } r_1 = 0 \\ &C_{z3}v_{11}(\chi = M) + C_{z4}v_{12}(\chi = M) + v_{z13}(\chi = M) = 0 \qquad \text{for : } r_1 = h_1 \end{aligned} \tag{43}$$

If the limits (41) are accounted for the set of equations (43) yields the following solutions :

$$C_{i3} = -\frac{v_{i13}(\chi = h_1 N)}{v_{11}(\chi = h_1 N)} \quad , \quad C_{i4} = 0 \quad \text{for : } i = \varphi, z \tag{44}$$

The general solutions of the oil velocity components (15), (14) at making use of the solutions (25), (35), (36), can be presented in the following form :

$$v_{\varphi 1} = C_{\varphi 1}v_{01}(\chi) + C_{\varphi 2} + v_{\varphi 03}(\chi,\varphi,z_1) + \frac{Des}{t_1}\left[C_{\varphi 3}v_{11}(\chi) + C_{\varphi 4}v_{12}(\chi) + v_{\varphi 13}(\chi,\varphi,z_1)\right] + O\left(\frac{Des}{t_1}\right)^2 \tag{45}$$

$$v_{z1} = C_{z1}v_{01}(\chi) + C_{z2} + v_{z03}(\chi,\varphi,z_1) + \frac{Des}{t_1}\left[C_{z3}v_{11}(\chi) + C_{z4}v_{12}(\chi) + v_{z13}(\chi,\varphi,z_1)\right] + O\left(\frac{Des}{t_1}\right)^2 \tag{46}$$

If $t_1 \to \infty$ then $N \to 0$, hence $\chi \equiv r_1 N \to 0$.

For further analysis it is worthwhile to find the following limits :

$$\lim_{\chi \to 0, N \to 0} N^2 v_{11}(\chi) = \lim_{\chi \to 0} N^2 \chi e^{-\chi^2} = 0 \tag{47}$$

$$\lim_{\chi \to 0, N \to 0} N^2 v_{12}(\chi) = \lim_{\chi \to 0, N \to 0} N^2 \chi e^{-\chi^2} \cdot \int_{\delta}^{\chi} \left(\frac{1}{\chi_1^2} e^{\chi_1^2} \right) d\chi_1 = 0 \tag{48}$$

for : $0 \le \chi_1 \le h_1 N$, $0 < t_1 < \infty$, $0 \le r_1 \le h_1$, $-1 \le z_1 \le +1$, $0 < \varphi < 2\pi$

VALUES OF OIL VELOCITY AND PRESSURE AT NON-STATIONARY NEWTONIAN LUBRICATION

If viscoelastic properties of oil are neglected, then on the basis of the solutions (45), (46) the oil velocity components in the φ and z directions, at non-stationary flow, are of the following form :

$$v_{\varphi 0\Sigma}(\varphi, r_1, z_1, t_1) = +1 - \left\{1 - \frac{\sqrt{\pi}}{2N^2}\frac{\partial p_{10}}{\partial \varphi}\Omega(\chi = Nh_1)\right\}\frac{\operatorname{erf}(r_1 N)}{\operatorname{erf}(h_1 N)} - \frac{\sqrt{\pi}}{2N^2}\frac{\partial p_{10}}{\partial \varphi}\Omega(\chi = Nr_1) \tag{49}$$

$$v_{z0\Sigma}(\varphi, r_1, z_1, t_1) = \frac{\sqrt{\pi}}{2N^2}\frac{\partial p_{10}}{\partial z_1}\Omega(\chi = Nh_1)\frac{\operatorname{erf}(r_1 N)}{\operatorname{erf}(h_1 N)} - \frac{\sqrt{\pi}}{2N^2}\frac{\partial p_{10}}{\partial z_1}\Omega(\chi = Nr_1) \tag{50}$$

for : $0 \le t_1 < \infty$, $0 \le r_1 \le h_1$, $-1 \le z_1 \le 1$, $0 < \varphi < 2\pi$, $0 \le \chi_2 \le \chi_1 \le \chi \equiv r_1 N \le h_1 N \equiv M$, $h_1 = h_1(\varphi, z_1)$

The oil velocity components (49), (50) are now inserted to the continuity equation (12) and next the equation is integrated respective to the variable r_1.

The oil velocity component $v_{r0\Sigma}$ in the gap height direction is not equal to zero on the cylindrical journal surface due to impulse displacements of the shaft. Therefore by applying the condition $v_{r0\Sigma} = Str\partial h_1/\partial t_1$ for $r_1 = 0$, the following form of this oil velocity component is obtained :

$$v_{r0\Sigma}(\varphi, r_1, z_1, t_1) = -\int_0^{r_1} \frac{\partial v_{\varphi 0\Sigma}}{\partial \varphi} dr_2 - \frac{1}{L_1^2}\int_0^{r_1} \frac{\partial v_{z0\Sigma}}{\partial z_1} dr_2 + Str\frac{\partial h_1}{\partial t_1} \tag{51}$$

for : $0 \le t_1 < \infty$, $0 \le r_2 \le r_1 \le h_1$, $-1 \le z_1 \le +1$, $0 < \varphi < 2\pi$, $0 \le \chi_2 \le \chi_1 \le \chi \equiv r_1 N \le h_1 N \equiv M$

The oil velocity component $v_{r0\Sigma}$ equals zero on the sleeve surface. Integrating the continuity equation (12) along the direction r and applying the boundary condition (32) for $r_1 = h_1$ to the oil velocity component in the gap height direction, and making use of the conditions (29) one obtains the equation :

$$\frac{\partial}{\partial \varphi}\int_0^{h_1} v_{\varphi 0\Sigma} dr_1 + \frac{1}{L_1^2}\frac{\partial}{\partial z_1}\int_0^{h_1} v_{z0\Sigma} dr_1 = Str\frac{\partial h_1}{\partial t_1} \tag{52}$$

The solutions (49) ÷ (50) are now inserted to the equation (52). One then obtains the following modified Reynolds equation :

$$\frac{\sqrt{\pi}}{2N^2}\frac{\partial}{\partial\varphi}\left\{\left[\frac{\int_0^{h_1}\operatorname{erf}(r_1N)dr_1}{\operatorname{erf}(h_1N)}\Omega(\chi=Nh_1)-\int_0^{h_1}\Omega(\chi=Nr_1)dr_1\right]\frac{\partial p_{10}}{\partial\varphi}\right\}+$$

$$+\frac{\sqrt{\pi}}{2N^2L_1^2}\frac{\partial}{\partial z_1}\left\{\left[\frac{\int_0^{h_1}\operatorname{erf}(r_1N)dr_1}{\operatorname{erf}(h_1N)}\Omega(\chi=Nh_1)-\int_0^{h_1}\Omega(\chi=Nr_1)dr_1\right]\frac{\partial p_{10}}{\partial z_1}\right\}= \tag{53}$$

$$=-\int_0^{h_1}\left[1-\frac{\operatorname{erf}(r_1N)}{\operatorname{erf}(h_1N)}\right]dr_1+Str\frac{\partial h_1}{\partial t_1}$$

for : $0\le r_2\le r_1\le h_1$, $0\le\varphi<2\pi$, $-1\le z_1<+1$, $0\le t_1<\infty$, $0\le\chi_1\le\chi\le h_1N$, $0\le N(t_1)=0.5(Res/t_1)^{0.5}<\infty$

The modified Reynolds equation (53) defines an unknown pressure function $p_{10}(\varphi, z_1, t_1)$. If the dimensionless time t_1 approaches infinity, i.e. the coefficient N approaches zero, then the equation (53) approaches the classical Reynolds equation (see App. 2) :

$$\frac{\partial}{\partial\varphi}\left(h_1^3\frac{\partial p_{10}}{\partial\varphi}\right)+\frac{1}{L_1^2}\frac{\partial}{\partial z_1}\left(h_1^3\frac{\partial p_{10}}{\partial z_1}\right)=6\frac{\partial h_1}{\partial\varphi}-12Str\frac{\partial h_1}{\partial t_1} \tag{54}$$

for : $0\le\varphi<2\pi$, $-1\le z_1<+1$

The dimensionless time-dependent height of the bearing gap height, at accounting for its periodical disturbances, may be described by the following relationship :

$$h_1=[1+\lambda\cdot\cos\varphi+s\cdot z\cdot\cos(\varphi)]\cdot f(t_1)\ ;\ f(t_1)=[1+c\cdot\exp(-t_o\cdot t_1\cdot\omega_o)] \tag{55}$$

where : $s=\frac{L}{\psi}\tan(\gamma)$- skew coefficient.

The symbol ω_o stands for an angular velocity given in $[s^{-1}]$ which describes the disturbances in the gap height direction for unsteady oil flow through the cylindrical bearing gap height, and "c" stands for a coefficient used to control values of gap height changes. If c- value is positive the bearing gap height is increased, if negative - the bearing gap height is decreased relative to the classical gap height. If t_1 approaches infinity then the gap height equation (55) approaches the classical gap height equation independent on time during stationary motion.

PRESSURE CORRECTIONS FOR VISCOELASTIC OIL PROPERTIES

Particular solutions of oil velocity components in the directions φ and z_1 due to viscoelastic properties in non-stationary motion are contained in the solutions (14) , (16) multiplied by the term $DeStr/t_1$. By making use of (38), (39), (44) and the boundary conditions (42), the corrections of the oil velocity components (35) , (36) can be transformed to the following forms :

$$\frac{Des}{t_1}v_{\varphi1\Sigma}(\varphi,z_1,r_1,t_1)=\frac{4\beta}{\rho\varepsilon^2}Nr_1e^{-r_1^2N^2}\left\{\frac{\partial p_{11}}{\partial\varphi}\left[\int_{r_1N}^{h_1N}\chi\Omega_1(\chi)d\chi+\right.\right.$$

$$+\frac{N^2}{2}\left(h_1^2-r_1^2\right)\Omega_1(\chi=h_1N)\left.\right]+\frac{\partial p_{10}}{\partial\varphi}\left[\int_{r_1N}^{h_1N}\Omega_2(\chi)d\chi-\Omega_1(\chi=h_1N)\int_0^{h_1N}\chi_1e^{-\chi^2}\Omega_2(\chi)d\chi+\right.$$

$$\left.+\Omega_1(\chi=r_1N)\int_0^{r_1N}\chi_1e^{-\chi^2}\Omega_2(\chi)d\chi\right]-\frac{2}{\sqrt{\pi}\operatorname{erf}(h_1N)}\frac{\partial p_{10}}{\partial\varphi}\left[\int_{r_1N}^{h_1N}\Omega_1(\chi)\Omega_3(\chi)\Omega(\chi)d\chi+\right. \tag{56}$$

$$\left.\left.-\Omega_1(\chi=h_1N)\int_0^{h_1N}\Omega_3(\chi)\Omega(\chi)d\chi+\Omega_1(\chi=r_1N)\int_0^{r_1N}\Omega_3(\chi)\Omega(\chi)d\chi\right]\right\}+$$

$$-\frac{8\beta N^2r_1e^{-r_1^2N^2}}{\sqrt{\pi}\rho\varepsilon^2\operatorname{erf}(h_1N)}\left[\Omega_1(\chi=h_1N)\int_0^{h_1N}\Omega_3(\chi)d\chi-\Omega_1(\chi=r_1N)\int_0^{r_1N}\Omega_3(\chi)d\chi-\int_{r_1N}^{h_1N}\Omega_1(\chi)\Omega_3(\chi)d\chi\right]$$

$$\frac{Des}{t_1}v_{z1\Sigma}(\varphi,z_1,r_1,t_1)=\frac{4\beta}{\rho\varepsilon^2}\frac{1}{L_1^2}Nr_1e^{-r_1^2N^2}\left\{\frac{\partial p_{11}}{\partial z_1}\left[\int_{r_1N}^{h_1N}\chi\Omega_1(\chi)d\chi+\right.\right.$$

$$+\frac{N^2}{2}\left(h_1^2-r_1^2\right)\Omega_1(\chi=h_1N)\left.\right]+\frac{\partial p_{10}}{\partial z_1}\left[\int_{r_1N}^{h_1N}\Omega_2(\chi)d\chi-\Omega_1(\chi=h_1N)\int_0^{h_1N}\chi e^{-\chi^2}\Omega_2(\chi)d\chi+\right.$$

$$\left.+\Omega_1(\chi=r_1N)\int_0^{r_1N}\chi e^{-\chi^2}\Omega_2(\chi)d\chi\right]-\frac{2}{\sqrt{\pi}erf(h_1N)}\frac{\partial p_{10}}{\partial z_1}\left[\int_{r_1N}^{h_1N}\Omega_1(\chi)\Omega_3(\chi)\Omega(\chi)d\chi+\right.$$

$$\left.\left.-\Omega_1(\chi=h_1N)\int_0^{h_1N}\Omega_3(\chi)\Omega(\chi)d\chi+\Omega_1(\chi=r_1N)\int_0^{r_1N}\Omega_3(\chi)\Omega(\chi)d\chi\right]\right\} \tag{57}$$

where :

$$\Omega_1(\chi)\equiv\int_\delta^\chi\frac{1}{\chi_1^2}e^{\chi_1^2}d\chi_1\ ,\ \Omega_2(\chi)\equiv\left(\chi+\frac{\chi^2}{2}\right)\left(2\chi e^{-\chi^2}\int_0^\chi e^{\chi_1^2}d\chi_1-1\right)\ ,\ \Omega_3(\chi)\equiv\chi^2(\chi+2)e^{-\chi^2} \tag{58}$$

and : $0\le t_1<\infty$, $0\le r_2\le r_1\le h_1$, $-1\le z_1\le 1$, $0<\varphi<2\pi$, $0\le\chi_1\le\chi\equiv r_1N\le h_1N\equiv M$

The corrections (56) , (57) are now inserted to the continuity equation (12) and then both its sides are integrated respective to the variable r.

From the viscoelastic oil properties it results that the corrections of the oil velocity component along the gap height must equal zero on the journal surface at $r_1 = 0$. Hence the correction of the oil velocity component along the gap height is as follows :

$$v_{r1\Sigma}(\varphi,z_1,r_1,t_1)=\frac{\partial}{\partial\varphi}\left(\int_0^{r_1}v_{\varphi1\Sigma}(\varphi,z_1,r_1,t_1)\,dr_1\right)+\frac{1}{L_1^2}\frac{\partial}{\partial z_1}\left(\int_0^{r_1}v_{z1\Sigma}(\varphi,z_1,r_1,t_1)\,dr_1\right) \tag{59}$$

The velocity vector corrections cannot change the boundary conditions (31) , (32) which are assumed on the journal and sleeve surfaces in the direction of the bearing gap height. Therefore the oil velocity vector corrections in this direction are equal to zero on the sleeve surface at $r_1=h_1$. By applying this condition to the solution (59) the modified Reynolds equation can be obtained :

$$\frac{\partial}{\partial\varphi}\left\{\frac{\partial p_{11}}{\partial\varphi}\left[\int_0^{h_1}r_1e^{-r_1^2N^2}\left(\int_{r_1N}^{h_1N}\chi\Omega_1(\chi)\,d\chi-r_1^2\Omega_1(\chi=r_1N)\right)dr_1+\frac{1}{4}\left(1-e^{-h_1^2N^2}\right)h_1^2\Omega_1(\chi=h_1N)\right]\right\}+$$

$$+\frac{1}{L_1^2}\frac{\partial}{\partial z_1}\left\{\frac{\partial p_{11}}{\partial z_1}\left[\int_0^{h_1}r_1e^{-r_1^2N^2}\left(\int_{r_1N}^{h_1N}\chi\Omega_1(\chi)\,d\chi-r_1^2\Omega_1(\chi=r_1N)\right)dr_1+\frac{1}{4}\left(1-e^{-h_1^2N^2}\right)h_1^2\Omega_1(\chi=h_1N)\right]\right\}=$$

$$=\frac{2N}{erf\left(Nh_1\right)}\int_0^{h_1}r_1e^{-r_1^2N^2}\left[\Omega_1(\chi=r_1N)\int_0^{h_1N}\Omega_3(\chi)d\chi-\Omega_1(\chi=r_1N)\int_0^{r_1N}\Omega_3(\chi)d\chi-\int_{r_1N}^{h_1N}\Omega_1(\chi)\Omega_3(\chi)d\chi\right]dr_1+$$

$$+\frac{2}{\sqrt{\pi}erf(h_1N)}\frac{\partial}{\partial\varphi}\left\{\frac{\partial p_{10}}{\partial\varphi}\left[\int_0^{h_1}r_1e^{-r_1^2N^2}\left(\int_{r_1N}^{h_1N}\Omega_1(\chi)\,\Omega_3(\chi)\,\Omega(\chi)\,d\chi+\right.\right.\right. \tag{60}$$

$$\left.\left.+\Omega_1(\chi=r_1N)\int_0^{r_1N}\Omega_1(\chi)\,\Omega_3(\chi)\,\Omega(\chi)\,d\chi\right)dr_1-\frac{1-e^{-h_1^2N^2}}{2N^2}\Omega_1(\chi=h_1N)\int_0^{h_1N}\Omega_1(\chi)\,\Omega_3(\chi)\,\Omega(\chi)\,d\chi\right]\right\}+$$

$$+\frac{2}{\sqrt{\pi}erf(h_1N)}\frac{1}{L_1^2}\frac{\partial}{\partial z_1}\left\{\frac{\partial p_{10}}{\partial z_1}\left[\int_0^{h_1}r_1e^{-r_1^2N^2}\left(\int_{r_1N}^{h_1N}\Omega_1(\chi)\,\Omega_3(\chi)\,\Omega(\chi)\,d\chi+\right.\right.\right.$$

$$\left.\left.+\Omega_1(\chi=r_1N)\int_0^{r_1N}\Omega_1(\chi)\,\Omega_3(\chi)\,\Omega(\chi)\,d\chi\right)dr_1-\frac{1-e^{-h_1^2N^2}}{2N^2}\Omega_1(\chi=h_1N)\int_0^{h_1N}\Omega_1(\chi)\,\Omega_3(\chi)\,\Omega(\chi)\,d\chi\right]\right\}+$$

$$-\frac{\partial}{\partial\varphi}\left\{\frac{\partial p_{10}}{\partial\varphi}\left[\int_0^{h_1}r_1 e^{-r_1^2N^2}\left(\int_{r_1N}^{h_1N}\Omega_2(\chi)\,d\chi+\Omega_1(\chi=r_1N)\int_0^{h_1N}\Omega_2(\chi)\,\chi e^{-\chi^2}d\chi\right)dr_1+\right.\right.$$
$$\left.\left.-\frac{1-e^{-h_1^2N^2}}{2N^2}\Omega_1(\chi=h_1N)\int_0^{h_1N}\Omega_2(\chi)\,\chi e^{-\chi^2}d\chi\right]\right\}+ \qquad (60)$$
$$-\frac{1}{L_1^2}\frac{\partial}{\partial z_1}\left\{\frac{\partial p_{10}}{\partial z_1}\left[\int_0^{h_1}r_1 e^{-r_1^2N^2}\left(\int_{r_1N}^{h_1N}\Omega_2(\chi)\,d\chi+\Omega_1(\chi=r_1N)\int_0^{h_1N}\Omega_2(\chi)\,\chi e^{-\chi^2}d\chi\right)dr_1+\right.\right.$$
$$\left.\left.-\frac{1-e^{-h_1^2N^2}}{2N^2}\Omega_1(\chi=h_1N)\int_0^{h_1N}\Omega_2(\chi)\,\chi e^{-\chi^2}d\chi\right]\right\}$$

for : $0 \le r_2 \le r_1 \le h_1$, $0 \le \varphi < 2\pi$, $-1 \le z_1 < +1$, $0 \le t_1 < \infty$, $0 \le \chi_1 \le \chi \le h_1N$, $0 \le N(t_1) = 0.5(Res/t_1)^{0.5} < \infty$

The modified Reynolds equation (60) determines unknown functions $p_{11}(\varphi, z_1, t_1)$ of the corrections of pressure values, resulting from viscoelastic oil properties during non-stationary motion.

NUMERICAL CALCULATIONS

The dimensionless distributions of values of the pressure p_{10} and its corrections p_{11}, p_{12}, ... in the lubrication area are determined by means of the Reynolds equations (53) , (60) with using the gap height (55). On the boundary of the area, dimensional values of the pressure and its corrections obtain the value of the atmospheric pressure p_{at}. The lubrication area and the gap height are shown in Fig.2. In order to determine a dimensional value of the gap height the dimensionless gap height indicated in Fig.2 should be multiply by the radial clearance ε. The lubrication area is defined by the following inequalities : $0 \le \varphi \le \pi$, $-1 \le z_1 \le 1$.

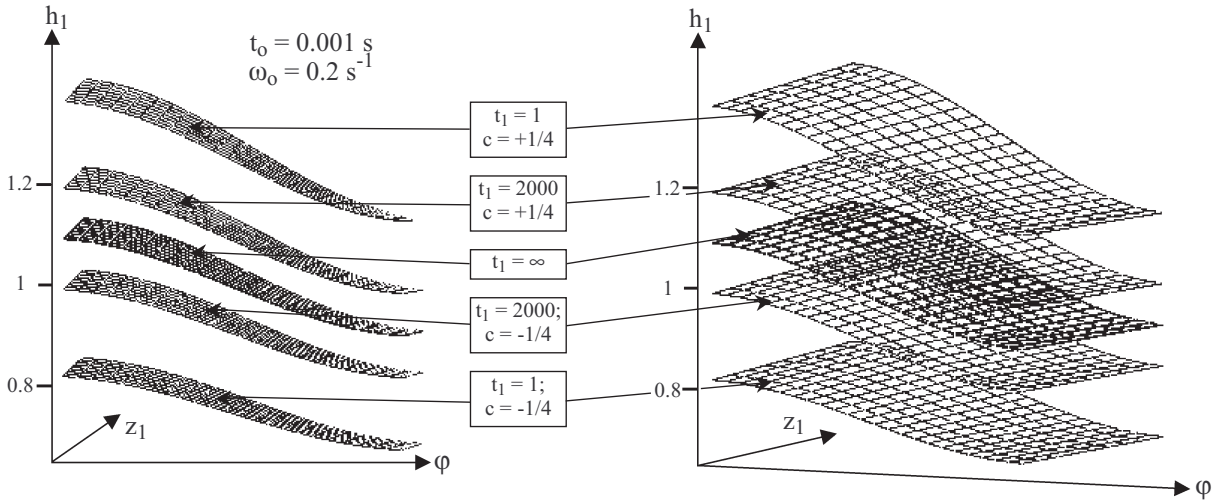

Fig. 2. *The example lubrication area with the time-variable height of lubrication bearing gap*

The values of the dimensionless time t_1 increasing from 1 to 2000 and even more express the time of departing from the instant of impulse occurrence of the force acting on friction unit. The impulse which causes the gap height decreasing was denoted with the negative value of the gap height change coefficient c = -1/4, and that causing the gap height increasing – with the positive value of that coefficient c = 1/4.

In order to calculate definite hydrodynamic pressure values the following input data were assumed :

- relative radial clearance : $\psi = 10^{-3}$
- oil viscosity : $\eta_o = 0.03$ [Pa·s]
- oil pseudo-viscosity coefficient : $\beta = 6\cdot10^{-4}$ [Pa·s^2]
- oil density : $\rho = 900$ [kg/m^3]
- shaft angular speed : $n = 1500$ [rpm]
- relative excentricity : $\lambda = 0.5$
- shaft radius : $R = 0.08$ [m]
- dimensionless bearing length : $L_1 = 1$
- skewness coefficient : $s = 0.05$
- angular speed of sleeve perturbation : $\omega_o = 0.2$ [s^{-1}]
- characteristic time : $t_o = 0.001$ [s]
- time intervals : $t_1 = 1 ; 100 ; 10000 ; \infty$

For the so assumed data and on the basis of the Reynolds equation (53) the dimensionless values of pressure distribution were numerically determined for the gap height defined by the equation (55) with the use of the method of finite differences and the software Mathcad 11 (Fig. 3, 4, 5, 6). In order to obtain real dimensional distributions of pressure values, the calculated dimensionless values of pressure distributions should be multiplied by the dimensional coefficient $UR\eta_o/\varepsilon^2$. The distributions of dimensionless hydrodynamic pressure values were presented for the dimensionless time intervals $t_1 = 1$; $t_1 = 100$; $t_1 = 10000$; $t_1 = \infty$ and the bearing gap height change coefficient c = ± 1/4.

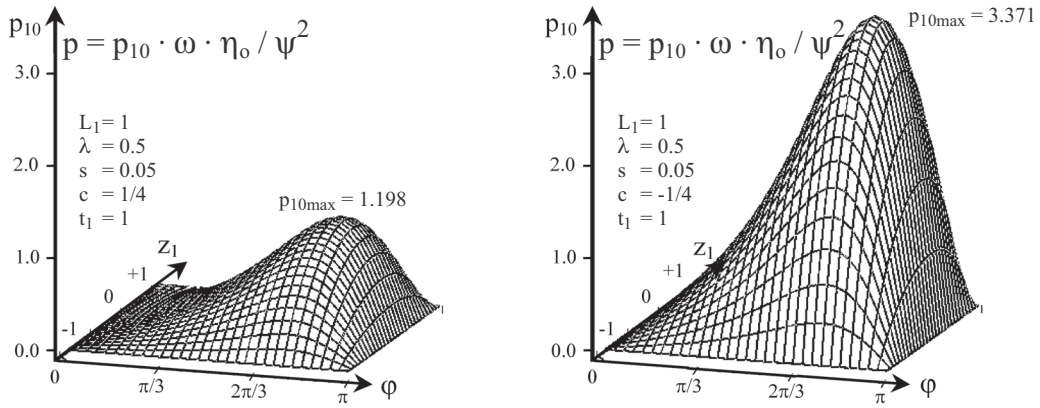

Fig. 3. *Distributions of the dimensionless hydrodynamic pressure in the cylindrical bearing gap for the dimensionless time t_1=1 counted from the impulse instant and for the gap height change coefficient c = +1/4 (lubrication gap height increased due to impulse load), and for c = -1/4 (lubrication gap height decreased due to impulse load) at accounting for a skew of the journal*

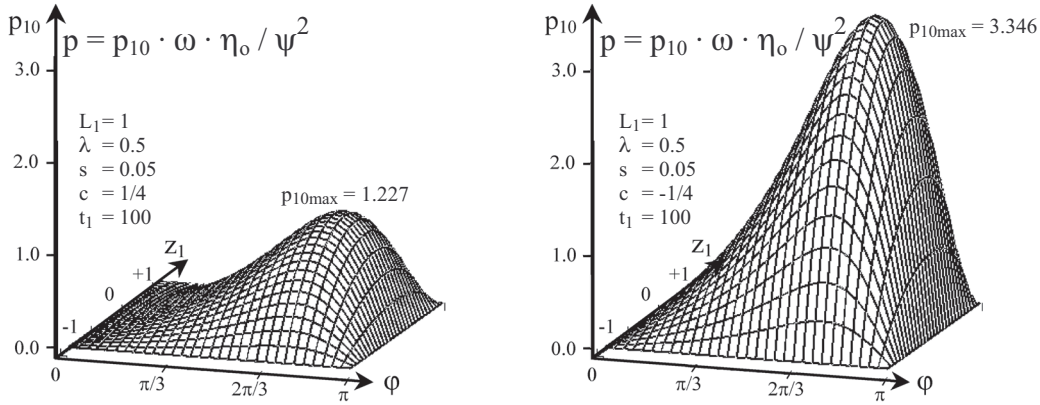

Fig. 4. *Distributions of the dimensionless hydrodynamic pressure in the cylindrical bearing gap for the dimensionless time t_1=100 counted from the impulse instant and for the gap height change coefficient c = +1/4 (lubrication gap height increased due to impulse load), and for c = -1/4 (lubrication gap height decreased due to impulse load) at accounting for a skew of the journal*

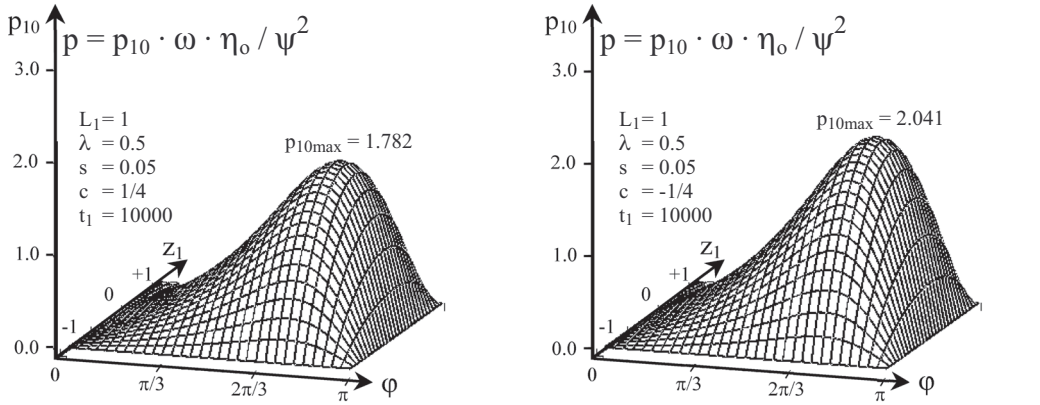

Fig. 5. *Distributions of the dimensionless hydrodynamic pressure in the cylindrical bearing gap for the dimensionless time t_1=10000 counted from the impulse instant and for the gap height change coefficient c = +1/4 (lubrication gap height increased due to impulse load), and for c = -1/4 (lubrication gap height decreased due to impulse load) at accounting for a skew of the journal*

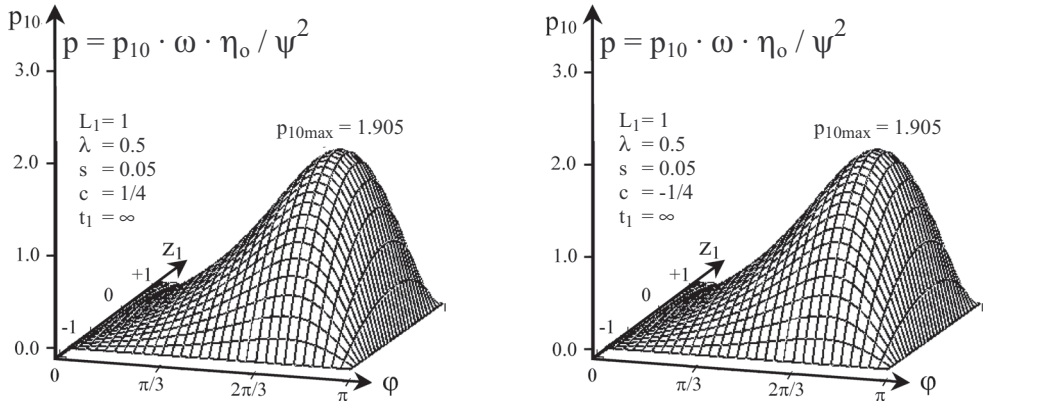

Fig. 6. *Distributions of the dimensionless hydrodynamic pressure in the cylindrical bearing gap for the dimensionless time $t_1 = \infty$ counted from the impulse instant and for the gap height change coefficient c = +1/4 (lubrication gap height increased due to impulse load), and for c = -1/4 (lubrication gap height decreased due to impulse load) at accounting for a skew of the journal*

For the same data on the basis of the equation (60) the numerical calculations of the dimensionless values of hydrodynamic pressure corrections which result from oil viscoelastic properties, were performed. Their results are presented in Fig. 7, 8, 9 for the dimensionless time intervals $t_1 = 1, 2, 10$. For $t_1 = 100$, $t_1 = 10000$ and $t_1 = \infty$, the calculations of dimensionless values of the hydrodynamic pressure corrections were also performed, but they have not been attached here as being negligible. To obtain dimensional values of the pressure corrections the dimensionless values shown in Fig. 7, 8, 9, should be multiplied by the dimensional coefficient $UR\eta_o/\varepsilon^2$.

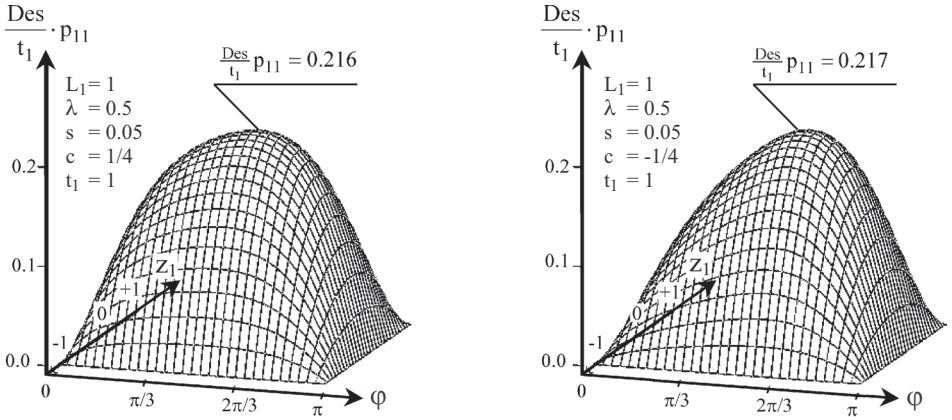

Fig.7. *Distributions of the dimensionless values of the hydrodynamic pressure corrections resulting from viscoelastic properties of oil in the cylindrical bearing gap for the dimensionless time $t_1 = 1$ counted from the impulse occurrence instant and for the gap height change coefficient $c = +1/4$ (lubrication gap height increased due to impulse load), and for $c = -1/4$ (lubrication gap height decreased due to impulse load) at accounting for a skew of the journal*

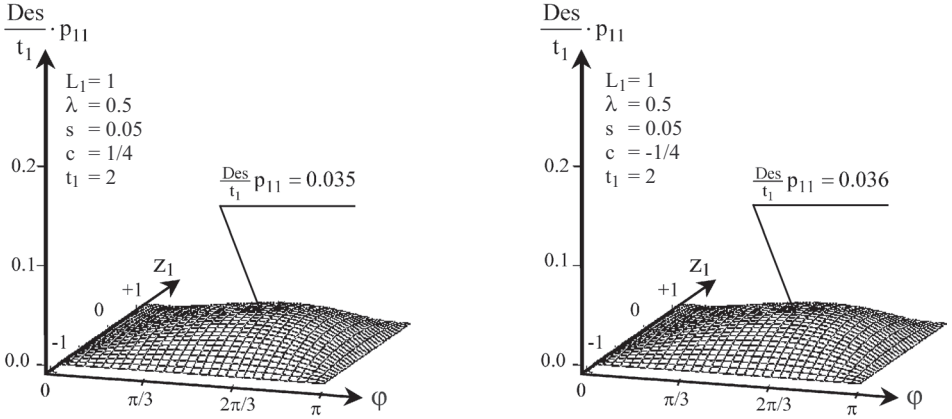

Fig.8. *Distributions of the dimensionless values of the hydrodynamic pressure corrections resulting from viscoelastic properties of oil in the cylindrical bearing gap for the dimensionless time $t_1 = 2$ counted from the impulse occurrence instant and for the gap height change coefficient $c = +1/4$ (lubrication gap height increased due to impulse load), and for $c = -1/4$ (lubrication gap height decreased due to impulse load) at accounting for a skew of the journal*

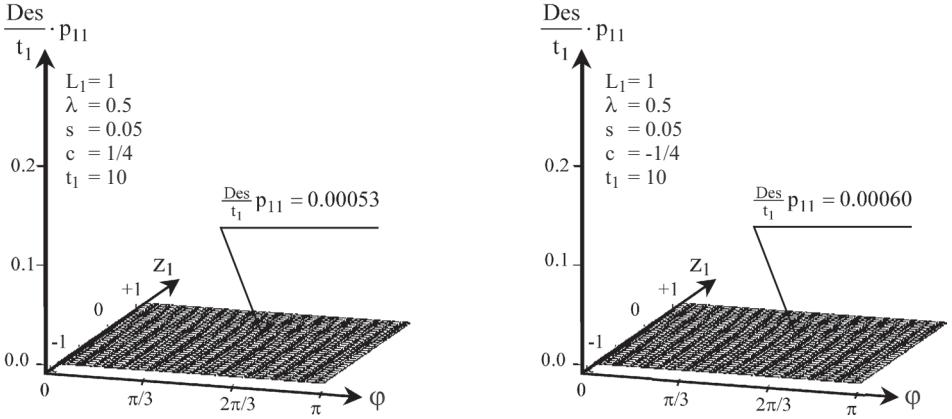

Fig.9. *Distributions of the dimensionless values of the hydrodynamic pressure corrections resulting from viscoelastic properties of oil in the cylindrical bearing gap for the dimensionless time $t_1 = 10$ counted from the impulse occurrence instant and for the gap height change coefficient $c = +1/4$ (lubrication gap height increased due to impulse load), and for $c = -1/4$ (lubrication gap height decreased due to impulse load) at accounting for a skew of the journal*

In Fig. 6 one can observe that when a load impulse occurs sufficiently far in time from the impulse occurrence instant, i.e. when $t_1 \to \infty$, then the distributions of pressure values approach the pressure distribution identical as regards its values and shape, both at the impulse increasing the gap height $c > 0$ and that decreasing the gap height $c < 0$, which can be also achieved from the classical Reynolds equation (54).

From the analysis of the pressure corrections (due to viscoelastic oil properties) it results that only in the initial instant $t_1 = 1$ after impulse occurrence (Fig.7) the corrections really influence the total pressure value. At the so assumed time instant $t_1 = 1$ the share of the corrections of pressure p_{11} in the value of the basic pressure p_{10} amounts to about 6% (at the gap height decreased due to impulse load, $c = -1/4$) and to about 18% (at that gap height increased due to impulse load, $c = +1/4$). The values were calculated for the relevant maximum values shown in Fig. 3 and 7.

DISCUSSION OF RESULTS AND CONCLUSIONS

- Numerical analysis of hydrodynamic pressure values during the unsteady impulse loading of radial slide cylindrical bearings reveals that in the first time interval counted from the instant of impulse load occurrence very high changes of the hydrodynamic pressure may appear, and also very high changes of bearing loads in comparison with their load carrying capacities which shall occur at no impulse load.
- In the case if due to an impulse load the journal changes its location relative to the sleeve in such a way that the lubrication gap height increases (left column of Fig. 3, 4, 5 and 6) then the bearing will suffer sudden drop of its load carrying capacity by a few dozen percent. As time runs after the impulse load occurrence the hydrodynamic pressure in the bearing gap height increases up to its value occurring under regular load (without any impulse).
- In the case when an impulse load results in decreasing the gap height (right column of Fig.3, 4, 5, 6) then an increase of pressure values appears in the initial phase of impulse loading and next, as time runs, the pressure decreases down to the hydrodynamic pressure value relevant for the bearing under regular load (without any impulse).
- The mixed case may also happen when the journal displaces itself due to simultaneous occurrence of two impulses of opposite tendencies leading to the decreasing and increasing of the gap height relative to its initial location. Then, rises and drops of hydrodynamic pressure in comparison to its initial value, may happen. Such hydrodynamic pressure changes may lead to an accelerated wear of elements of the cylindrical slide friction units in question.
- The accounting for the impulse-load-induced pressure changes in designing the cylindrical slide friction units, would contribute to elimination of engine failures resulting from seizure of cylindrical slide bearings in the service conditions in which impulse loads often occur. Transport safety would be this way improved.

Appendix 1

$$\frac{\partial}{\partial t_1}=\frac{\partial}{\partial\chi}\frac{\partial\chi}{\partial t_1}=-\frac{1}{4}\sqrt{Res}\,\frac{r_1}{t_1\sqrt{t_1}}\frac{\partial}{\partial\chi}=-\frac{\chi}{2t_1}\frac{\partial}{\partial\chi}$$
$$\frac{\partial^2}{\partial r_1^2}=\frac{\partial}{\partial r_1}\left(\frac{\partial}{\partial r_1}\right)=\frac{\partial}{\partial\chi}\left(\frac{\partial}{\partial\chi}\frac{\partial\chi}{\partial r_1}\right)\frac{\partial\chi}{\partial r_1}=\frac{Res}{4t_1}\frac{\partial^2}{\partial\chi^2} \tag{A1.1}$$

$$\frac{\partial^3}{\partial t_1\partial r_1^2}=\frac{\partial}{\partial t_1}\left(\frac{Res}{4t_1}\frac{\partial^2}{\partial\chi^2}\right)=-\frac{Res}{4t_1^2}\frac{\partial^2}{\partial\chi^2}+\frac{Res}{4t_1}\frac{\partial}{\partial\chi}\left(\frac{\partial^2}{\partial\chi^2}\right)\frac{\partial\chi}{\partial t_1}=-\frac{Res}{4t_1^2}\left(\frac{\partial^2}{\partial\chi^2}+\frac{\chi}{2}\frac{\partial^3}{\partial\chi^3}\right) \tag{A1.2}$$

Appendix 2

$$\lim_{N\to0}\frac{\sqrt{\pi}}{2N^2}\Omega(\chi=h_1N)\equiv\lim_{N\to0}\frac{\sqrt{\pi}}{2N^2}\left[\int_0^{h_1N}\exp(\chi^2)\operatorname{erf}(\chi)d\chi-\operatorname{erf}(h_1N)\int_0^{h_1N}\exp(\chi^2)d\chi\right]=$$
$$=\lim_{N\to0}\frac{1}{N^2}\left\{\int_0^{h_1N}\left[\exp(\chi^2)\int_0^{\chi}\exp(-\chi_1^2)d\chi_1\right]d\chi-\left(\int_0^{h_1N}\exp(-\chi^2)d\chi_2\right)\left(\int_0^{h_1N}\exp(\chi^2)d\chi\right)\right\}= \tag{A2.1}$$
$$\overset{H}{=}-\lim_{N\to0}\frac{h_1\int_0^{Nh_1}\exp(\chi^2)d\chi}{2N\exp(h_1^2N^2)}\overset{H}{=}-\frac{h_1^2}{2}\lim_{N\to0}\frac{\exp(h_1^2N^2)}{\exp(h_1^2N^2)+2h_1^2N^2\exp(h_1^2N^2)}=-\frac{h_1^2}{2}$$

Analogically :

$$\lim_{N\to0}\frac{\sqrt{\pi}}{2N^2}\left[\int_0^{r_1N}\exp(\chi^2)\operatorname{erf}(\chi)d\chi-\operatorname{erf}(r_1N)\int_0^{r_1N}\exp(\chi^2)d\chi\right]=-\frac{r_1^2}{2} \tag{A2.2}$$

$$\text{and}:\ \lim_{N\to0}\frac{\operatorname{erf}(r_1N)}{\operatorname{erf}(h_1N)}=\frac{r_1}{h_1} \tag{A2.3}$$

The equation (53) at N→0 approaches the following form :

$$\frac{\partial}{\partial\varphi}\left\{\left[\left(-\frac{h_1^2}{2}\right)\int_0^{h_1}\frac{r_1}{h_1}dr_1-\int_0^{h_1}\left(-\frac{r_1^2}{2}\right)dr_1\right]\frac{\partial p_{10}}{\partial\varphi}\right\}+$$
$$+\frac{1}{L_1^2}\frac{\partial}{\partial z_1}\left\{\left[\left(-\frac{h_1^2}{2}\right)\int_0^{h_1}\frac{r_1}{h_1}dr_1-\int_0^{h_1}\left(-\frac{r_1^2}{2}\right)dr_1\right]\frac{\partial p_{10}}{\partial z_1}\right\}=-\frac{\partial}{\partial\varphi}\left[\int_0^{h_1}\left(1-\frac{r_1}{h_1}\right)dr_1\right] \tag{A2.4}$$

After realisation of the calculations the classical Reynolds equation is obtained in the form of (54) for a cylindrical system.

Acknowledgement

This scientific work has been financed by Polish State Committee for Scientific Research during the years 2001-2003.

NOMENCLATURE

$\mathbf{a}$	- acceleration vector [m/s^2]
$\mathbf{A}_1$	- Rivlin-Ericksen strain tensors [s^{-1}]
$\mathbf{A}_2$	- Rivlin-Ericksen strain tensors [s^{-2}]
b	- a half of bearing length [m]
c	- coefficient for controllling gap height changes
C_{z1} , C_{z2} , C_{z3} , C_{z4} , $C_{\varphi 1}$, $C_{\varphi 2}$, $C_{\varphi 3}$, $C_{\varphi 4}$	- integration constants
De	- Deborah number
h	- gap height in the cylindrical bearing [m]
h_1	- dimensionless gap height
$\mathbf{I}$	- unit tensor
$\mathbf{L}$	- tensor of oil velocity vector gradient [s^{-1}]
$\mathbf{L}^T$	- tensor with matrix transpose [s^{-1}]
$\mathbf{L}_1$	- dimensionless bearing length
N	- dimensionless number
$O\left(\frac{Des}{t_1}\right)^2$	- estimate of all remaining corrections of velocity and pressure components
p	- pressure [Pa]
p_o	- characteristic value of hydrodynamic pressure [Pa]
p_1	- total dimensionless hydrodynamic pressure
p_{10} , p_{11} , p_{12}	- dimensionless corrections of hydrodynamic pressure
P	- load [N]
r	- radial coordinate [m]
r_1 , r_2	- dimensionless radial coordinate
R	- radius of cylindrical journal [m]
Re	- Reynold's number
s	- skew coefficient
$\mathbf{S}$	- stress tensor [Pa]
Str	- Strouhal number
t	- time [s]
t_o	- characteristic time [s]
t_1 , t_2	- dimensionless time
U	- tangential journal velocity [m/s]
$\mathbf{v}$	- velocity vector [m/s]
v_φ , v_r , v_z	- dimensional values of tangential, radial and axial components of velocity vector, respectively [m/s]
$v_{\varphi 1}$, v_{r1} , v_{z1}	- dimensionless values of tangential, radial and axial components of velocity vector, respectively
$v_{\varphi 0\Sigma}$, $v_{r0\Sigma}$, $v_{z0\Sigma}$	- dimensionless components of oil velocity vector, without accounting for changes due to disturbing impulse
$v_{\varphi 1\Sigma}$, $v_{r1\Sigma}$, $v_{z1\Sigma}$, $v_{\varphi 2\Sigma}$, $v_{r2\Sigma}$, $v_{z2\Sigma}$	- dimensionless corrections of oil velocity vector components, resulting from disturbing impulse impact on a bearing at sufficiently close instant from the impulse occurrence
v_{10} , v_{20}	- parts of dimensionless velocity vector components, dependent on shaft rotation, without accounting for disturbing impulse action
v_{11} , v_{12}	- parts of dimensionless velocity vector components, dependent on shaft rotation, with accounting for disturbing impulse action
$v_{\varphi 03}$, v_{z03}	- parts of dimensionless velocity vector components, resulting from pressure gradient influence, without accounting for disturbing impulse action
$v_{\varphi 13}$, v_{z13}	- parts of dimensionless velocity vector components, resulting from pressure gradient influence, with accounting for disturbing impulse action
z	- longitudinal coordinate [m]
z_1	- dimensionless longitudinal coordinate
α , β	- pseudo-viscosity constants of oil [Pa·s^2]
γ	- skew angle
δ	- a value close zero
ε	- radial clearance
η_o	- characteristic value of oil dynamic viscosity [Pa·s]
λ	- relative eccentricity
ρ	- oil density [kg/m3]
φ	- tangential coordinate
χ , χ_1 , χ_2	- dimensionless coordinates
ψ	- relative radial clearance
ω	- angular journal velocity [s^{-1}]
ω_o	- angular speed of sleeve perturbation [s^{-1}]
Ω , Ω_1 , Ω_2 , Ω_3	- auxiliary functions

BIBLIOGRAPHY

1. Astarita G., Marrucci G.: *Principles of non-Newtonian Fluid Mechanics*. McGraw Hill Co. London, 1974
2. Böhme G.: *On Steady Streaming in Viscoelastic Liquids*. Journal of Non-Newtonian Fluid Mechanics, No 44, 1992
3. Girtler J.: *Availability of Sea Transport Means*. Archives of Transport. Quarterly of Polish Academy of Sciences.Vol.9, iss. 3-4. Warszawa, 1997
4. Girtler J.: *Semi-Markov Model of Changes of Safety of Movements of Sea Ship and Aircrafts*. Archives of Transport. Quarterly of Polish Academy of Sciences, Vol.11, iss. 1-2, Warszawa, 1999
5. Knopp K.: *Unfinite series* (in Polish translated from German) PWN. 1956
6. Miszczak A.: *Theoretical study on influence of non-Newtonian oils on operational parameters of stationary loaded radial slide bearings* (in Polish). Doctorate thesis. Mining-Metalurgical Academy, Kraków, 1998
7. Teipel I., Waterstraat A.: *Nichtnewtonische Schmiermittel im Radialgleitlager*. Konstruktion, Vol. 32, No 10, 1980
8. Tipei N.: *Theory of Lubrication*. California, W. A. Gross Stanford. University Press. 1962
9. Truesdell. C. A.: *First Course in Rational Continuum Mechanics*, John Hopkins University/Baltimore, Maryland 1972, Piervonaczalnyj Kurs Racionalnoj Mechaniki. MIR. Moskva, 1975
10. Wierzcholski K. Pytko S.: *Calculations of cylindrical slide bearings lubricated with oils of non-Newtonian properties* (in Polish). Zagadnienia Eksploatacji Maszyn. Quarterly of Polish Academy of Sciences, Vol. 25, iss. 4 (84), 1990
11. Wierzcholski K.: *Mathematical methods in hydrodynamic theory of lubrication*. Technical University of Szczecin, Monography No 511. Szczecin, 1993
12. Wierzcholski K., Krasowski P.: *Slide journal bearing lubrication for oil dynamic viscosity changes by pressure and magnetic field*. Proc. of II International Scientific Technical Conference : Explo-Diesel & Gas Turbione 01. Vol. 1. Gdańsk--Międzyzdroje-Kopenhaga, 2001
13. Wierzcholski K : *Ferromagnetic Turbulent Lubrication for Thermoelasticity Deformations of Bearing Gap*. The Fifth International Congress on Thermal Stresses and Related Topics. Virginia Polytechnic Institute and State University Blacksburg. 2003 Proceedings WA4-3 pp.WA4-3-1-WA4-3-4, Virginia USA
14. Zahorski S.: *Effect of small amplitude harmonic vibrations on viscoelastic flows in a plane slider bearing*. Arch. Mech, Vol. 34, No 1, 1982
15. Zhang Z., Jiang X.: *Analysis of Cylindrical Journal Bearing With Viscoelastic Bush*. Transaction of the ASME, Journal of Tribology, Vol. 112, 1990

CONTACT WITH THE AUTHOR

Andrzej Miszczak, D.Sc., M.E.
Gdynia Maritime University,
Faculty of Marine Engineering
81-225 Gdynia, ul. Morska 81-87
e-mail: miszczak@am.gdynia.pl

Seating of machines and devices on foundation chocks cast of EPY resin compound

A valuable book written by Prof. Karol Grudziński and Dr Eng Wiesław Jaroszewicz, has been recently published.

The book presents a modern method for the seating of marine and land-based machines and devices on chocks cast of EPY resin compound specially developed for this purpose. General requirements referring to the seating of machinery on foundations (especially those used in shipbuilding) are listed together with relevant evaluation criteria. The properties of resin compounds used for foundation chocks, the background of chocking arrangement design and the techniques used for casting the chocks in place are also outlined.

Many examples of so installed machines and devices are described, illustrating various possible applications of EPY compound to the seating of new machinery and the repairs of existing one. The results and descriptions of research aimed at finding solutions for many practical problems in this field, constituting a scientific basis of the methods developed for the seating of machines on their foundations, are also given.

The book of 186 pages consists
of the six topical chapters :

1. Characteristics and types of chocking arrangements used for ship machinery
2. The resin compounds used for ship machinery foundation chocks
3. Design of machinery chocking arrangements with EPY compound chocks
4. The technology of machinery seating on EPY compound chocks
5. Applications of EPY compound chocks for the seating of machinery - practical examples
6. Research on resin compounds used for foundation chocks (this chapter occupies amost a half of the book and is illustrated with 74 fotoghaphies and drawings)

The attached bibliography contains 83 references. The book is ended with "The chronological list of research reports concerning Polish resin compounds used for foundation chocks, and their practical application for the seating of machinery"(containing 132 items both published and unpublished).

The book is addressed to designers and shipbuilding technology specialists as well as the engineers and technicians dealing with the design, modernisation and execution of various heavy machinery installations on land. It may also be of use for the scientific workers and students of the university faculties engaged in the fields of shipbuilding and offshore technology, machinery design and maintenance, industrial constructions and the building of roads and bridges.

The first of the authors of the book, Prof. Karol Grudziński, has worked at the Chair of Mechanics and Principles of Mechanical Design, Faculty of Mechanical Engineering, Technical University of Szczecin. The area of his scientific interests covers the mechanics of machines, mechanics of contact between real surfaces and tribology, with main focus on experimental research, modelling and calculations of constructional joints. The results of his research has been presented in this book. Prof. Karol Grudziński is an author and co-author of about 200 scientific papers.

Dr Eng Wiesław Jaroszewicz, the other author of the book, has been angaged in the machinery seating technology since the early 1980s. He has owned the Marine Service Jaroszewicz company since 1990, which has developed the EPY resin compound and carried out machinery seating operations based on its use. He is a co-author of many scientific publications, patents and reports. Over 7500 shipboard and land machines have been installed in the years of 1974 - - 2002 under his supervision and with his cooperation, including over 1500 main engines of ships. The practical expertise gained during this multi-year activity has been comprehensively presented in the book in question.

This English edition of the book
is a translation from the Polish edition of 2002.
The book assigned with ISBN 83-87377-94-5 mark, has been published by ZAPOL Publishing Company, Szczecin.

Fatigue "safe-life" criterion for metal elements under multiaxial constant and periodic loads

Janusz Kolenda
Gdańsk University of Technology
Naval University of Gdynia

ABSTRACT

Periodic stress with Cartesian components given in the form of Fourier series is considered. To account for the mean stress effect the generalised Soderberg criterion for ductile materials is employed. An equivalent stress with synchronous components is defined by means of the equivalence conditions based on the average strain energy of distortion. The fatigue "safe-life" design criterion is formulated which covers the conditions of both static strength and fatigue safety and includes material constants that have simple physical interpretation, can be determined by uniaxial tests, are related directly to the applied loads and can reflect material anisotropy.

Key words : design criteria, multiaxial loading, periodic stress, mean stress effect

INTRODUCTION

Machinery parts and structural elements are frequently subjected to simultaneous action of constant and cyclic stresses. In marine floating objects, constant stresses are mainly caused by deadweight and hydrostatic pressure, whereas those encountered in machinery systems are produced by torque, thrust, centrifugal force, etc. In the present paper also cyclic stresses induced by time-varying loads of periodic character are considered.

Each Cartesian component of the cyclic stress can be characterised by its mean value and parameters of its alternating part. It is important to remember that the total strength of an engineering element is altered if residual stresses are present. Since residual stresses have a similar influence on the fatigue behaviour of materials as that of mechanically imposed constant stresses of the same magnitude [1], no distinction will be made between constant, mean and residual stresses.

In order to ensure a fatigue safe life (theoretically infinite) under bending stress of mean value c_b and amplitude a_b two approaches can be indicated [2]. The first is based on the condition :

$$a_b^* \le F_b \tag{1}$$

where :

$$a_b^* = a_b + \psi_b c_b \tag{2}$$

is the amplitude of the equivalent zero mean stress,

$\psi_b = 0.1 \div 0.2$ - the asymmetry sensitivity index at bending
F_b - the fatigue limit under fully reversed bending.

Analogous conditions can be applied in the case of axial force or torsional moment.

In the second approach the effect of mean stress is described by a "failure diagram" or by one of the empirical equations, such as Goodman's, Gerber's, Soderberg's or Bagci's equation, depending on a given situation [2÷5]. In the following the Soderberg's equation for ductile materials is used in the form :

$$B = F_b\left(1 - \frac{c_b}{R_e}\right) \tag{3}$$

where :
B - maximum allowable stress amplitude in fatigue "safe-life" design under asymmetric bending
R_e - tensile yield strength.

BACKGROUND

Introducing the safety factor :

$$f = \frac{B}{a_b} \tag{4}$$

and partial safety factors :

$$f_s = \frac{R_e}{c_b} \qquad f_d = \frac{F_b}{a_b} \tag{5}$$

one obtains from (3) :

$$f = f_d\left(1 - f_s^{-1}\right) \tag{6}$$

So, the design criterion reads :

$$f \geq 1 \tag{7}$$

i.e.,

$$f_s^{-1} + f_d^{-1} \leq 1 \tag{8}$$

Here the subscript "s" stands for static and "d" for dynamic parts of the applied stress.

Obviously, the condition (1) concerns exclusively fatigue endurance of the material subjected to combined constant and cyclic loads, whereas satisfaction of (8) guarantees that not only the static strength of the material is not exceeded but also that the combination of constant and cyclic loads will not lead to fatigue failure. Another essential point is that the partial safety factors in (8) can be analysed and/or influenced separately. Therefore (1) and (2) is not used hereunder.

The explicit forms of (8) read :

$$\frac{c_b}{R_e} + \frac{a_b}{F_b} \leq 1 \tag{9}$$

for asymmetric bending,

$$\frac{c_a}{R_e} + \frac{a_a}{F_a} \leq 1 \tag{10}$$

for asymmetric push-pull force, and

$$\frac{c_t}{R_t} + \frac{a_t}{F_t} \leq 1 \tag{11}$$

for asymmetric torsional moment, where :

$$R_t = \frac{1}{\sqrt{3}} R_e \tag{12}$$

$$F_t = \frac{1}{\sqrt{3}} F_b \tag{13}$$

applicable for steels [4].

Here the subscripts "a", "b" and "t" denote axial, bending and torsional load cases, respectively, and F_a is the fatigue limit under symmetric tension-compression.

The aim of this paper is to extend the use of eqation (8) to multiaxial non-zero mean periodic stresses. For this purpose it is necessary to determine a reduced stress, equivalent in terms of fatigue performance of the material under the multiaxial stress. For example, in the case of in-phase stress with Cartesian components :

$$\sigma_i(t) = c_i + a_i \sin \omega t \qquad i = x, y, z, xy, yz, zx \tag{14}$$

such reduced stress can be calculated for ductile metals by means of the average-distortion-energy strength hypothesis [6] as :

$$\sigma_{eq}(t) = c_{eq} + a_{eq} \sin \omega t \tag{15}$$

where its mean value and amplitude are given by :

$$c_{eq} = \left[\begin{array}{l} c_x^2 + c_y^2 + c_z^2 - c_x c_y - c_y c_z + \\ - c_z c_x + 3\left(c_{xy}^2 + c_{yz}^2 + c_{zx}^2\right) \end{array} \right]^{1/2} \tag{16}$$

$$a_{eq} = \left[\begin{array}{l} a_x^2 + a_y^2 + a_z^2 - a_x a_y - a_y a_z + \\ - a_z a_x + 3\left(a_{xy}^2 + a_{yz}^2 + a_{zx}^2\right) \end{array} \right]^{1/2} \tag{17}$$

For the sake of brevity the stress components $\sigma_z(t)$, $\sigma_{yz}(t)$ and $\sigma_{zx}(t)$ are dropped. It is noteworthy that in the case of out-of-phase stress components :

$$\sigma_i(t) = c_i + a_i \sin\left(\omega t + \beta_i\right) \qquad i = x, y, xy \tag{14a}$$

the average-distortion-energy strength hypothesis yields :

$$a_{eq} = \left[a_x^2 + a_y^2 - a_x a_y \cos\left(\beta_x - \beta_y\right) + 3a_{xy}^2 \right]^{1/2} \tag{17a}$$

According to the aforementioned hypothesis, the reduced stress (15) corresponds to that in an element of the specimen under uniaxial tension-compression test. Consequently, (10) can be used, which leads to the partial safety factors :

$$f_s = \frac{R_e}{c_{eq}} \qquad f_d = \frac{F_a}{a_{eq}} \tag{18}$$

and to the fatigue "safe-life" criterion :

$$\begin{aligned} &\frac{1}{R_e}\left(c_x^2 + c_y^2 - c_x c_y + 3c_{xy}^2\right)^{1/2} + \\ &+ \frac{1}{F_a}\left(a_x^2 + a_y^2 - a_x a_y + 3a_{xy}^2\right)^{1/2} \leq 1 \end{aligned} \tag{19}$$

With (12), (16) and (18) one gets :

$$f_s = \left[\frac{1}{R_e^2}\left(c_x^2 + c_y^2 - c_x c_y\right) + \frac{1}{R_t^2} c_{xy}^2 \right]^{-1/2} \tag{20}$$

Since normal stress components can be produced by loads of different mode (tension, compression, bending), and shear stress components – by torsion or shear, and the material may exhibit certain degree of anisotropy, the following modification of (20) is suggested [7] :

$$f_s = \left\{ \begin{array}{l} \dfrac{1}{R_e^2}\left[\begin{array}{l} \left(\dfrac{R_e}{R_x} c_x\right)^2 + \left(\dfrac{R_e}{R_y} c_y\right)^2 + \\ - \dfrac{R_e}{R_x} c_x \dfrac{R_e}{R_y} c_y \end{array} \right] + \\ + \dfrac{1}{R_t^2}\left(\dfrac{R_t}{R_{xy}} c_{xy}\right)^2 \end{array} \right\}^{-1/2} \tag{21}$$

Here R_x is the yield strength under static load relevant to the mean stress component c_x. The remaining material constants are defined analogously. Equation (21) gives :

$$f_s = \left[\sum_i \left(\frac{c_i}{R_i}\right)^2 - \frac{c_x c_y}{R_x R_y} \right]^{-1/2} \qquad i = x, y, xy \tag{22}$$

With (13) and (17), the equation (23), similar to (22), can be written for the partial safety factor f_d [8] :

$$f_d = \left[\sum_i \left(\frac{a_i}{F_i}\right)^2 - \frac{a_x a_y}{F_x F_y} \right]^{-1/2} \qquad i = x, y, xy \tag{23}$$

where F_i is the fatigue limit under fully reversed load relevant to the stress amplitude a_i. Equations (8), (22) and (23) yield the following criterion of fatigue "safe life" under combined multiaxial constant and in-phase loads [9] :

$$\left[\sum_i\left(\frac{c_i}{R_i}\right)^2-\frac{c_x c_y}{R_x R_y}\right]^{1/2}+\left[\sum_i\left(\frac{a_i}{F_i}\right)^2-\frac{a_x a_y}{F_x F_y}\right]^{1/2}\le 1 \tag{24}$$

Equation (24) may be called the generalised Soderberg criterion of an infinite fatigue life under non-zero mean in-phase stress.

EQUIVALENT STRESS UNDER MULTIAXIAL CONSTANT AND PERIODIC LOADS

Let us consider the stress with Cartesian components given by Fourier series :

$$\sigma_i(t)=c_i+\sum_{p=1}^{\infty}a_{ip}\sin\left(p\omega_0 t+\beta_{ip}\right)\qquad i=x,y,xy \tag{25}$$

where :

c_i - mean value of i-th stress component
a_{ip}, β_{ip} - amplitude and phase angle of p-th term in Fourier expansion of i-th stress component
$\omega_0 = 2\pi/T_0$ - fundamental circular frequency
T_0 - common period of the stress components.

Guided by the above presented criterion for the stress components (14), we shall try to model the stress components (25) by the equivalent stress components :

$$\sigma_i^{(eq)}(t)=c_i^{(eq)}+a_i^{(eq)}\sin\left(\omega_{eq}t+\varphi_i\right)\qquad i=x,y,xy \tag{26}$$

where :

$c_i^{(eq)}$ - mean value of i-th equivalent stress component
$a_i^{(eq)}, \varphi_i$ - amplitude and phase angle of i-th equivalent stress component
ω_{eq} - equivalent circular frequency.

For determination of parameters of the equivalent stress components the theory of energy transformation systems [10] is used. According to this theory, a reduced stress model and a given multiaxial stress can be regarded as equivalent in terms of fatigue life of the material if during the service life the internally and externally dissipated energies per unit volume in these two stress states are respectively equal. Under the assumption that the externally dissipated energy is proportional to the average strain energy of distortion, the following equivalence condition can be written [11] :

$$\frac{1}{T_o}\int_0^{T_o}\phi_{eq}(t)dt=\frac{1}{T_o}\int_0^{T_o}\phi(t)dt \tag{27}$$

where :

$$\phi_{eq}(t)=\frac{1+\nu}{3E}\left[\begin{array}{c}\left(\sigma_x^{(eq)}\right)^2+\left(\sigma_y^{(eq)}\right)^2+\\-\sigma_x^{(eq)}\sigma_y^{(eq)}+3\left(\sigma_{xy}^{(eq)}\right)^2\end{array}\right]$$

is the strain energy of distortion per unit volume in the equivalent stress state, and :

$$\phi(t)=\frac{1+\nu}{3E}\left(\sigma_x^2+\sigma_y^2-\sigma_x\sigma_y+3\sigma_{xy}^2\right)$$

is that in the actual stress state, and :

E - Young modulus
ν - Poisson's ratio.

If the condition (27) is fulfilled then also the following equations are satisfied :

$$\frac{1}{T_o}\int_0^{T_o}\left[\sigma_i^{(eq)}(t)\right]^2dt=\frac{1}{T_o}\int_0^{T_o}\sigma_i^2(t)dt \tag{28}$$

$$\frac{1}{T_o}\int_0^{T_o}\sigma_x^{(eq)}(t)\sigma_y^{(eq)}(t)dt=\frac{1}{T_o}\int_0^{T_o}\sigma_x(t)\sigma_y(t)dt \tag{29}$$

When : $\omega_{eq}=k\,\omega_0$ (30)

where : k - a natural number, is assumed
then (25) through (29) yield :

$$c_i^{(eq)}=c_i \tag{31}$$

$$a_i^{(eq)}=\left(\sum_{p=1}^{\infty}a_{ip}^2\right)^{1/2} \tag{32}$$

$$a_x^{(eq)}a_y^{(eq)}\cos\left(\varphi_x-\varphi_y\right)=\sum_{p=1}^{\infty}a_{xp}a_{yp}\cos\left(\beta_{xp}-\beta_{yp}\right) \tag{33}$$

Of course, in design for an infinite fatigue life the evaluation of equivalent circular frequency can be avoided.

FATIGUE "SAFE-LIFE" CRITERION

Having determined the parameters of equivalent stress components, one can make use of the criterion (24) which, in particular, is suitable also for non-zero mean stress with synchronous components of the form (26). In this instance one obtains :

$$\left[\sum_i\left(\frac{c_i^{(eq)}}{R_i}\right)^2-\frac{c_x^{(eq)}c_y^{(eq)}}{R_x R_y}\right]^{1/2}+\left[\sum_i\left(\frac{a_i^{(eq)}}{F_i}\right)^2-\frac{a_x^{(eq)}a_y^{(eq)}\cos\left(\varphi_x-\varphi_y\right)}{F_x F_y}\right]^{1/2}\le 1 \tag{34}$$

so that the fatigue "safe-life" design criterion for metal elements under multiaxial constant and periodic loads becomes :

$$\left[\sum_i\left(\frac{c_i}{R_i}\right)^2-\frac{c_x c_y}{R_x R_y}\right]^{1/2}+\left[\sum_i\sum_{p=1}^{\infty}\left(\frac{a_{ip}}{F_i}\right)^2-\frac{1}{F_x F_y}\sum_{p=1}^{\infty}a_{xp}a_{yp}\cos\left(\beta_{xp}-\beta_{yp}\right)\right]^{1/2}\le 1 \tag{35}$$

Its extension to three-dimensional cases is straightforward.

CONCLUSIONS

- The fatigue "safe-life" design criterion covering the conditions of both static strength and fatigue safety of metal elements under multiaxial constant and periodic loads, was formulated.
- The presented criterion includes material constants which : have simple physical interpretation, can be determined by uniaxial tests, are directly related to the applied loads, and can reflect the material anisotropy.

NOMENCLATURE

a_a , a_b , a_t - stress amplitude under asymmetric axial force, bending moment and torsional load, respectively
a_b^* - amplitude of the equivalent zero mean stress under asymmetric bending
a_i , c_i - amplitude and mean value of i-th stress component (i = x, y, z, xy, yz, zx)
a_{eq} , c_{eq} - amplitude and mean value of the equivalent stress, respectively
$a_i^{(eq)}$, $c_i^{(eq)}$ - amplitude and mean value of i-th equivalent stress component, respectively
a_{ip} - amplitude of p-th harmonic in Fourier expansion of i-th stress component
B - maximum allowable stress amplitude in design for an infinite fatigue life under asymmetric bending
c_a , c_b , c_t - mean stress value under axial force, bending moment and torsional load, respectively
E - Young modulus
f - safety factor
f_d , f_s - partial safety factors
F_a , F_b , F_t - fatigue limit under fully reversed tension-compression, bending and torsion, respectively
F_i - fatigue limit under fully reversed load relevant to the stress amplitude a_i
k - natural number
R_e - tensile yield strength
R_i - yield strength relevant to the mean stress component c_i
R_t - shear yield strength
t - time
T_0 - stress period
β_i - phase angle of i-th component of the out-of-phase stress
β_{ip} - phase angle of p-th harmonic in Fourier expansion of i-th stress component
ν - Poisson's ratio
σ_i - i-th stress component
σ_{eq} - equivalent stress
$\sigma_i^{(eq)}$ - i-th equivalent stress component
φ_i - phase angle of i-th equivalent stress component
ϕ , ϕ_{eq} - strain energy of distortion per unit volume in the actual and equivalent stress states, respectively
ψ_b - asymmetry sensitivity index in bending
ω - circular frequency
ω_0 - fundamental circular frequency of the actual stress
ω_{eq} - equivalent circular frequency

BIBLIOGRAPHY

1. Osgood C.C.: *Fatigue design*. Pergamon Press. Oxford, 1982
2. Kocańda S., Szala J.: *Fundamentals of fatigue calculations* (in Polish). PWN, Warszawa, 1997
3. Almar-Naess A. (Ed.): *Fatigue handbook. Offshore steel structures*. Tapir Publishers. Trondheim, 1985
4. Blake A. (Ed.): *Handbook of mechanics, materials and structures*. Wiley & Sons. New York, 1985
5. Hu Qiao, Xu Hao: *Two-parameter nominal stress approach*. Int. J. Fatigue, No 5, 1995
6. Kolenda J.: *Average-distortion-energy strength hypothesis*. Proc. of the 17th Symp. on Fatigue and Fracture Mechanics. Bydgoszcz-Pieczyska, 1998
7. Kolenda J.: *Generalised safety factor and reliability index in a multiaxial state of static stress*. Marine Technology Transactions, Vol. 3, 1992
8. Kolenda J.: *Safety factor and reliability index in a general state of cyclic stress*. Marine TechnologyTransactions, Vol. 3, 1992
9. Kolenda J.: *A new design criterion of steel elements at multiaxial constant and in-phase loadings*. Proc. of the 18th Symp. on Fatigue and Fracture Mechanics. Bydgoszcz--Pieczyska, 2000
10. Cempel C.: *Theory of energy transformation systems and their application in diagnostic of operating systems*. Applied Math. and Computer Sciences, No 3, 1993
11. Kolenda J.: *Application of the theory of energy transformation systems to fatigue assessment of steel elements under multiaxial periodic loading*. Marine Technology Transactions, Vol. 12, 2001

CONTACT WITH THE AUTHOR

Janusz Kolenda, Prof.,D.Sc.
Faculty of Ocean Engineering
and Ship Technology
Gdańsk University of Technology
Narutowicza 11/12
80-952 Gdańsk, POLAND
e-mail : sek7oce@pg.gda.pl

Conference

Maritime Traffic Engineering

On 20 and 21 November 2003, 10th International Conference devoted to problems of maritime traffic engineering was held in Świnoujście on the Baltic sea coast. It was organized by the Institute of Maritime Traffic Engineering, Maritime University of Szczecin.

The vast program of the Conference comprised 66 papers 6 of which were presented during the plenary session, and the remaining during 5 topical sessions.

The following papers were presented during the plenary session :

- *Extreme parameters of ships intended for entering the port of Świnoujście* - by S. Gucma and W. Ślączka (Maritime University of Szczecin)
- *Mathematical model of ship motion in canals and locks* by S. Zaikov, M. Lavrinovsky and V. Zaikov (State University for Water Communication, St. Petersburg)
- *Ship as intelligent machine* - by R. Śmierzchalski (Gdynia Maritime University)
- *On necessity of establishing a Polish Institute of Navigation following the example of similar institutions operating in neighbouring countries* - by A. Weintrit (Gdynia Maritime University)
- *The competences and duties of the officers in the charge of a navigational watch in the face of coming into operation of the ship's integrated control systems* by Z. Kopacz, W. Morgaś and J. Urbański (Naval University, Gdynia)
- *A method for the improving of location accuracy of objects with the use of teledetection data* - by J. Sanecki, A. Klewski, L. Cwojdziński, K. Maj and P. Kamieński (Military Engineering Academy, Warsaw)

The authors of the conference papers represented 15 scientific research centres including one of Slovakia and one of Russia. The greatest contribution to the conference materials (36 papers) was made by the authors of Maritime University of Szczecin. The conference became a comprehensive review of the interesting research projects concerning maritime traffic engineering, carried out in this university.

Kinematical control of motion of underwater vehicle in horizontal plane

Jerzy Garus
Naval University, Gdynia

ABSTRACT

In the paper presented is a method of designing a fuzzy-logic-based autopilot for control of horizontal motion of an unmanned underwater vehicle. The control system's synthesis was performed under the assumption that the vehicle can move with variable linear and angular velocities and the quantities possible to be measured are : position and orientation of the vehicle in the inertial reference system. The task of the autopilot was to minimize the mean squares of deviations from the motion trajectory given in the form of a broken line defined by the coordinates of successive turning points. To generate control signals three independent fuzzy PD controllers using the control principles based on the Mac Vicar-Whelan's standard base, were applied. For the linguistic variables of each controller appropriate fuzzy sets were selected and linear membership functions of trapezoidal and triangular form were defined. The presented results of the simulation tests performed for the remotely operated underwater vehicle „Ukwiał", with and without influence of disturbances resulting from sea current, confirm the proposed approach to be correct and effective.

Key words : Underwater vehicle, autopilot, fuzzy logic

INTRODUCTION

An increasing interest has been given to underwater robotics in the last years. Currently, it is common to use unmanned underwater vehicles (UUVs) to accomplish such missions as : inspection of coastal and off-shore structures, cable maintenance, as well as hydrographical and biological surveys. In the military field they are employed in such tasks as surveillance, intelligence gathering, torpedo recovery and mine counter measures. The main benefits of usage of the UUVs can be the possibility of removing a man from the dangers of the undersea environment, and of reduction in cost of exploration of underwater space.

There are various categories of the UUVs. The most often used are remotely operated vehicles (ROVs). The ROV is usually connected to a surface ship by a tether through which all communication is wired. The tether's drag influences motion of the vehicle and may produce significant disturbances and energy loss. The ROV is equipped with a power transmission system and controlled only by thrusters. Simultaneously the spatial station-keeping or tracking of the underwater vehicle is a difficult task for a human operator, hence a supervisory control has been developed to support its own intelligence and autonomy.

Automatic control of underwater vehicles is a complex problem due to their strongly coupled and highly nonlinear dynamic characteristics. Moreover, the dynamic characteristics can change depending on a chosen vehicle's configuration suitable to its mission. In order to cope with the difficulties the control system should be flexible. An interesting review of classical and modern techniques adopted to control the dynamic behaviour of unmanned underwater vehicles was presented in [1,3]. Nowadays fuzzy logic control systems have been successfully applied to a wide variety of mechanical systems [2,7,9]. The primary advantage of the fuzzy controllers is the possibility of easy incorporating heuristic knowledge of experts into a control strategy. In this paper a fuzzy autopilot for tracking control of the ROV is described.

TRACKING CONTROL

The general motion of a marine vehicle of 6 degrees of freedom (DOF) can be described by the following vectors [3] :

$$\begin{aligned} \eta &= [x, y, z, \phi, \theta, \psi]^T \\ \nu &= [u, v, w, p, q, r]^T \\ \tau &= [X, Y, Z, K, M, N]^T \end{aligned} \tag{1}$$

where :

- η - the position and orientation vector in the earth-fixed frame
- ν - the linear and angular velocity vector in the body-fixed frame
- τ - the forces and moments acting on the vehicle in the body-fixed frame.

The nonlinear dynamic equations of motion can be expressed in matrix form as [3] :

$$\mathbf{M}\dot{\nu} + \mathbf{C}(\nu)\nu + \mathbf{D}(\nu)\nu + \mathbf{g}(\eta) = \tau$$
$$\dot{\eta} = \mathbf{J}(\eta)\nu \qquad (2)$$

where :

M - inertia matrix (including added mass)
C(ν) - matrix of Coriolis and centripetal terms (including added mass)
D(ν) - hydrodynamic damping and lift matrix
g(η) - vector of gravitational forces and moments
J(η) - velocity transformation matrix.

Coordinate systems and tracking control

For the conventional ROVs a basic motion is the movement in horizontal plane with some variation due to diving. They operate in crab-wise manner with 4 DOF and small roll and pitch angles which can be neglected during normal operation. Therefore, it is purposeful to regard 3-dimensional motion of the vehicle as the superposition of the motion in the horizontal plane and that in the vertical plane. Farther in the paper only the movement of the vehicle in the horizontal plane is considered.

It is convenient to define three coordinate systems when analysing route tracking systems for the marine vehicle moving in horizontal plane (Fig.1) [6] :

- the global coordinate system $O_0X_0Y_0$ (the earth-fixed frame)
- the local coordinate system OXY (fixed to the body of the vehicle)
- the reference coordinate system $P_iX_iY_i$ (not fixed).

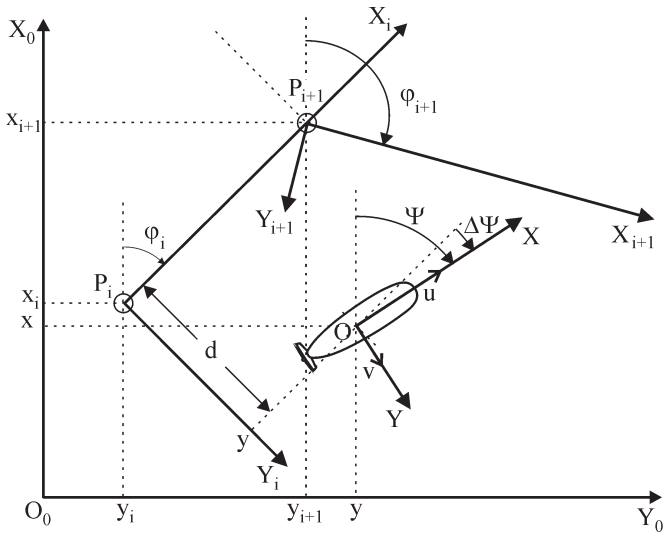

Fig. 1. *Coordinate systems used to describe tracking control of the underwater vehicle moving in the horizontal plane:* $O_0X_0Y_0$ *– global system,* OXY *– local system,* $P_iX_iY_i$ *– reference system*

The main task of the designed tracking control system is to minimize the distance of attitude of the vehicle's centre of gravity, d, to the desired trajectory under the following assumptions :

- the vehicle can move with variable linear velocities u, v, and angular velocity r
- the vehicle's position coordinates, x, y, and heading angle ψ are measurable
- the command signal τ consists of three components : *X* and *Y* - forces along X- and Y-axis, respectively, and *N* - moment around Z-axis
- a travel time is not given in advance, thus the navigation between two points is not constrained by time.

The tracking autopilot has to provide both track-keeping and course-keeping capabilities. Hence, the autopilot should minimize the mean squares of deviations "d", from a desired track, and Δψ deviations from a desired course:

$$J = \min_t \sum \left[d^2(t) + \lambda \Delta\psi^2(t) \right] \qquad (3)$$

where:

$$d(t) = -\sin(\Delta\psi)\left(x(t) - x_i\right) + \cos(\Delta\psi)\left(y(t) - y_i\right)$$

$$\varphi_i = \operatorname{arctg}\left[\frac{y_{i+1} - y_i}{x_{i+1} - x_i}\right]$$

Δψ(t) - angle between the track reference line and vehicle's centreline : $\psi(t) - \varphi_i$
ψ(t) - heading angle of the vehicle
λ - constant coefficient.

Each time the vehicle location x(t), y(t) at the instant t satisfies :

$$\left[x_{i+1} - x(t)\right]^2 + \left[y_{i+1} - y(t)\right]^2 \le \rho^2 \qquad (4)$$

where :

ρ - radius of circle of acceptance.

The next waypoint should be selected on the basis of the reference coordinate system (e.g. $P_{i+1}X_{i+1}Y_{i+1}$) and the vehicle's position should be updated in compliance with the new reference coordinate system.

Fuzzy control law

A fuzzy proportional derivative controller, adopted from [2], working in the configuration presented in Fig.2, has been designed for the tracking control.

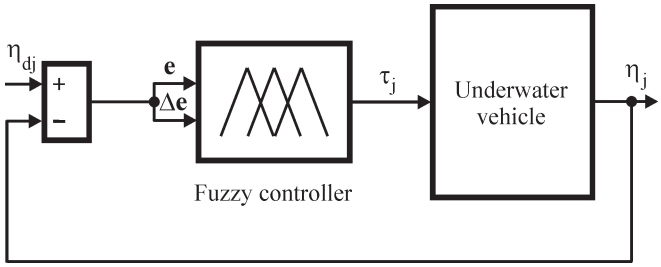

Fig. 2. *The assumed structure of the fuzzy controller*

The membership functions of fuzzy sets of the input variables : the error signal $e = \eta_{dj} - \eta_j$ and the derived change of error $\Delta e = \eta_j - \eta_{j-1}$, as well as the output variable : the command signal τ_j - for $j \in \{1, 2, 6\}$ - are shown in Fig.3.

Values of unknown parameters: x_e, $x_{\Delta e}$, x_S and x_M used in computer simulations are given in Tab.1. Evaluation of the parameters can be done by means of many optimisation techniques, classical or modern ones, e.g. Genetic Algorithms [4,5].

Tab. 1. The assumed membership function parameters

	Controller		
	position along X_0-axis	position along Y_0-axis	heading angle
x_e	0.14	0.19	0.39
$x_{\Delta e}$	0.87	0.63	0.52
x_M	0.25	0.40	0.38
x_S	0.89	0.74	0.65

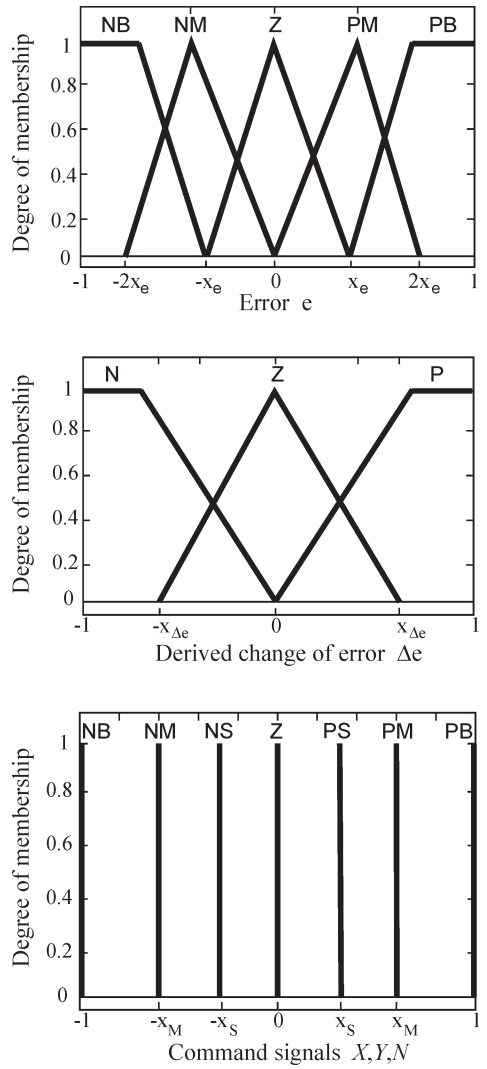

Fig. 3. *The assumed membership functions for fuzzy sets of : the error e, derived change of error Δe, and command signals X,Y,N.* ***Notation*** *: N - negative, Z - zero, P - positive, S - small, M - medium and B - big*

The chosen control rules, taken from the Mac Vicar-Whelan's standard base of rules [8], are given in Tab.2.

Tab. 2. The assumed base of rules

		Error signal e				
		NB	NM	Z	PM	PB
Derived change of error Δe	N	NB	NM	NS	Z	PS
	Z	NM	NS	Z	PS	PM
	B	NS	Z	PS	PM	PB
		Command signals *X,Y,N*				

SIMULATIONS

A simulation study of tracking control has been performed for an underwater vehicle „Ukwiał" designed and built by Gdańsk University of Technology for the Polish Navy. The ROV is an open, 1.5 m long frame robot controllable in 4 DOF, fitted with a propulsion system consisted of 6 thrusters.

The vehicle can move in horizontal plane by using four thrusters. Every thruster can generate thrust force up to ±250 N. It assures its speed up to u = ±1.2 m/s and v = ±0.6 m/s in X and Y direction, respectively. The autopilot in question consists of 3 independent controllers producing the command signals *X*, *Y* and *N* calculated on the basis of the proposed fuzzy law (under the constraints : $|X| \leq 500$ N, $|Y| \leq 150$ N and $|N| \leq 50$ Nm).

The structure of the proposed control system is presented in Fig.4.

Numerical simulations have been made to confirm validity of the proposed control algorithm under the following assumptions:

- the vehicle has to follow the desired route beginning from the position and orientation point : (x = 10 m, y = 10 m, ψ = 0°), passing the target waypoints : (10 m, 90 m, 90°), (30 m, 90 m, 0°), (30 m, 10 m, 270°), (60 m, 10 m, 0°) and ending at the point : (60 m, 90 m, 90°)
- the turning point is reached when the vehicle operates within the 1,5 m radius of circle of acceptance, ρ
- the initial conditions are the same.

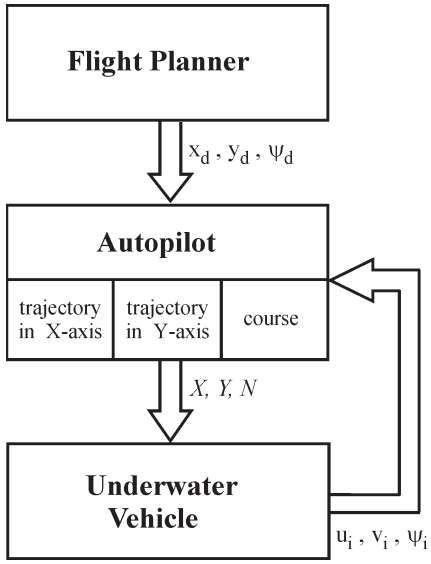

Fig. 4. *The block diagram of the track-keeping system* ***Notation*** *: index d - desired value*

The tracking control simulation results and the courses of command signals for no added environmental disturbances are shown in Fig.5. The real route and position of the vehicle almost coincides with those desired. Also the quality of course-keeping control is satisfactory (course deviations close to zero). In Fig.6 illustrated is an influence of sea current disturbances on the vehicle's route and course. A clear difference between the desired and real tracking curves is there observed. Although the errors of position and course are much bigger than in the previous case the autopilot is able to cope with the external disturbances and to reach the turning points with the commanded orientation. It should be noted that the last simulations were performed for the sea current speed increased to 0.35 m/s.

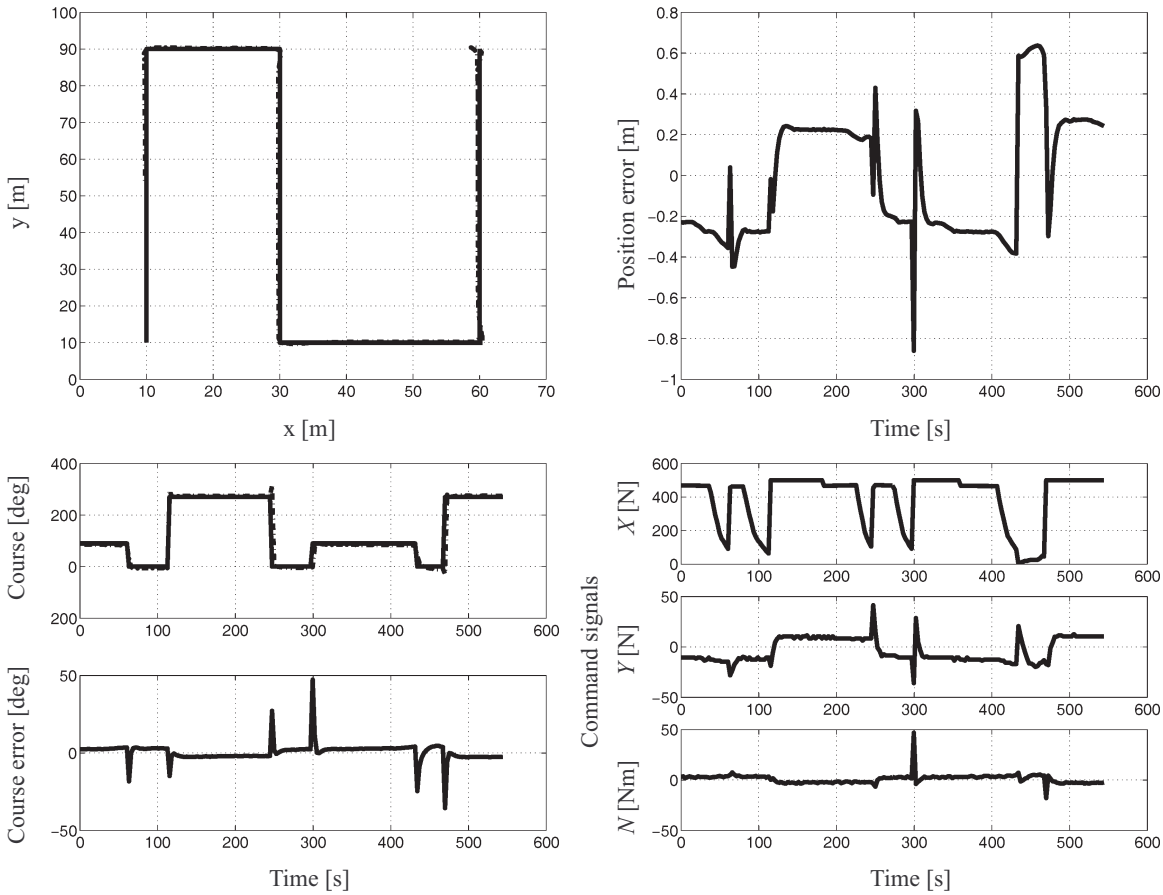

Fig. 5. *The vehicle's tracking curve and course deviations from the desired position and course, for the command signals without interaction of environmental disturbance*
Notation *: ——— desired –·–·– real*

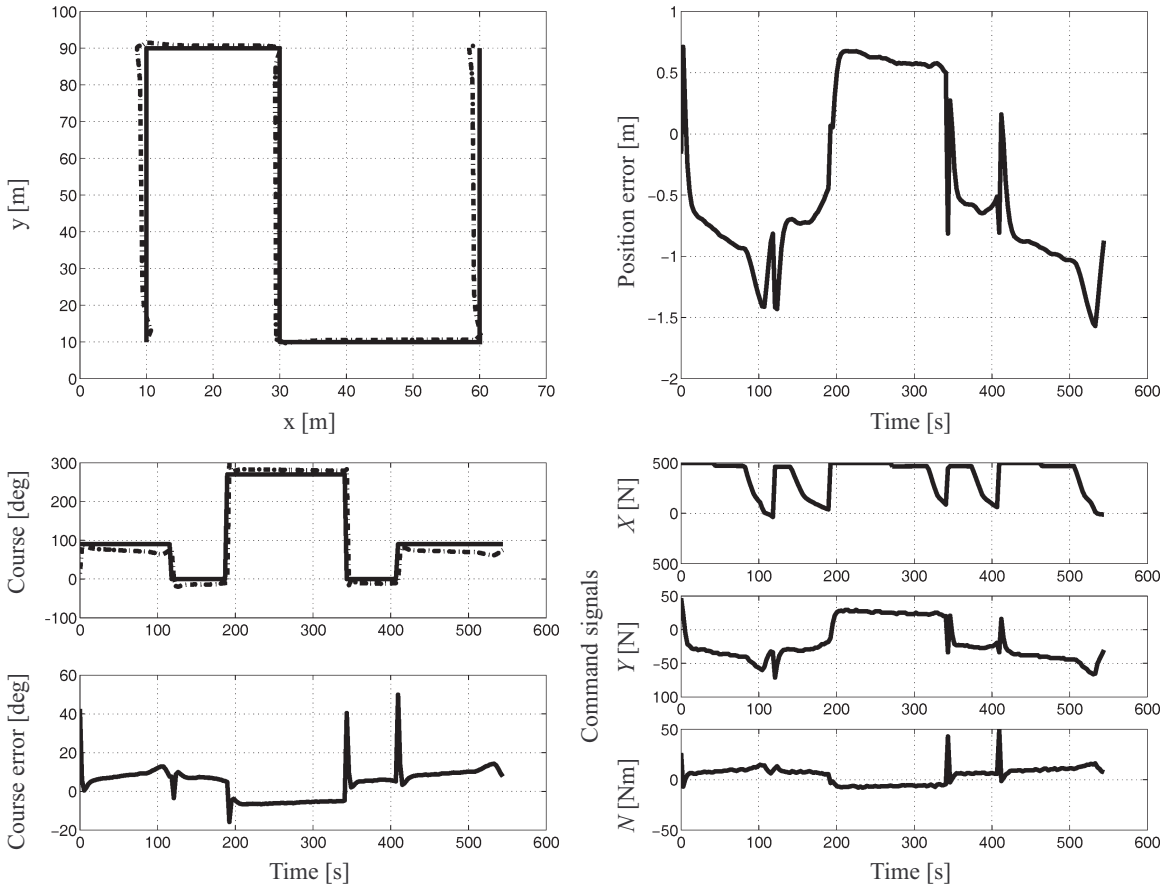

Fig. 6. *The vehicle's tracking curve and course deviations from the desired position and course, for the command signals under influence of the sea current of 0.35 m/s speed, and 135° direction angle*
Notation *: ——— desired –·–·– real*

This is comparable with the average speed of the vehicle. As it was expected, the guidance was very sensitive to the ratio of the vehicle speed and the current speed. It was observed that this ratio should not be smaller than 2, which is also confirmed in [6].

CONCLUSIONS

- In this paper the waypoint-tracking autopilot using fuzzy control, intended for underwater vehicles, has been described. The nonlinear model of the ROV „Ukwiał" was applied to carry out computer simulations.
- The simulation results obtained by using the control system design method based on three decoupling fuzzy controllers, showed the presented autopilot to be simple and useful for practical use.
- The main advantage of the proposed solution is its flexibility with regard to the vehicle's dynamic model, and its high performance at relatively large disturbances resulting from sea current.

NOMENCLATURE

$\mathbf{C}(\mathbf{v})$	- matrix of Coriolis and centripetal terms (including added mass)
d	- distance of attitude of the vehicle's centre of gravity from the desired trajectory
DOF	- degress of freedom
$\mathbf{D}(\mathbf{v})$	- hydrodynamic damping and lift matrix
e	- error signal
$\mathbf{g}(\eta)$	- vector of gravitational forces and moments
J	- quality index
$\mathbf{J}(\eta)$	- velocity transformation matrix
K	- moment around X- axis
$\mathbf{M}$	- inertia matrix (including added mass)
M	- moment around Y- axis
N	- moment around Z- axis
OXY	- local coordinate system (fixed to the body of the vehicle)
$O_0X_0Y_0$	- global coordinate system (the earth-fixed frame, inertial)
p	- angular velocity around X- axis
$P_iX_iY_i$	- reference coordinate system (not fixed, connected with trajectory of motion)
q	- angular velocity around Y- axis
r	- angular velocity around Z- axis
t	- time
u	- linear velocity along X-axis
v	- linear velocity along Y- axis
w	- linear velocity along Z- axis
x	- vehicle's position coordinate along X_0 - axis
x_e , $x_{\Delta e}$	- coordinates of membership functions of e and Δe, respectively, (along axis of abscissae)
x_S , x_M	- coordinates of membership functions of τ_j, (along axis of abscissae)
X	- force along X- axis
y	- vehicle's position coordinate along Y_0 - axis
Y	- force along Y- axis
z	- vehicle's position coordinate along Z_0 - axis
Z	- force along Z- axis
Δe	- derived change of error
$\Delta\psi$	- change of heading angle (deviation from a desired course)
η	- vehicle's position and orientation vector in the earth--fixed frame
θ	- vehicle's pitch angle
λ	- constant coefficient
ν	- linear and angular velocity vector in the body-fixed frame
ρ	- radius of circle of acceptance
τ	- forces and moments acting on the vehicle in the body--fixed frame
φ_i	- direction angle of i-th segment of trajectory
ϕ	- vehicle's roll angle
ψ	- vehicle's yaw (heading) angle

BIBLIOGRAPHY

1. Craven P. J., Sutton R., Burns R. S.: *Control strategies for unmanned underwater vehicles*. Journal of Navigation, No 51, 1998
2. Driankov D., Hellendoorn H., Reinfrank M.: *An introduction to fuzzy control.* Springer-Verlag. 1993
3. Fossen T.I.: *Guidance and control of ocean vehicles*. John Wiley and Sons. Chichester, 1994
4. Garus J.: *Genetic algorithms applied to designing of fuzzy controllers for underwater vehicle* (in Polish). Proc. of 14th National Conference of Automation. Zielona Góra, 2002
5. Goldberg D.E.: *Genetic algorithms in search, optimisation and machine learning.* Adison-Wesley. 1989
6. Hansen A.D.: *Predictive control and identification: application to steering dynamic.* Ph.D. Dissertation, Technical University of Denmark, Department of Mathematical Modelling. 1996
7. Kacprzyk J.: *Multistage fuzzy control.* John Wiley and Sons. Chichester. 1997
8. Mac Vicar-Whelan P.J.: *Fuzzy sets for man-machine interactions*. International Journal of Man-Machine Studies, No. 8, 1977
9. Yager R.R., Zadeh L.A.: *An introduction to fuzzy logic applications in intelligent systems.* Kluwer Academic Publishers, 1991

CONTACT WITH THE AUTHOR

Jerzy Garus
Department of Mechanical
and Electrical Engineering
Naval University
Śmidowicza 69
81-103 Gdynia, POLAND
e-mail : jgarus@amw.gdynia.pl

FOREIGN *conference*

A Hundred-Year Jubilee

On 7 July of the year 1903 – in accordance with the record in the commemorative book – the research establishment for water engineering and shipbuilding VWS (Versuchanstalt fuer Wasserbau und Schiffbau) officially commenced its activity in Berlin.

In the course of time it could boast of outstanding - in the worldwide scale - scientific and technical achievements in the domain of inland waterways, harbour engineering and shipbuilding.

On this special occasion the German society of naval architects and marine engineers STG (Schiffbautechnische Gesellschaft) held its general assembly on 19 - 22 November 2003 just in Berlin.

Its agenda contained , apart from its organizational part dealing with STG matters, the special session devoted to the achievements of the VWS, as well as the scientific conference carried out within 5 topical sessions.

Scientific workers of the Faculty of Ocean Engineering and Ship Technology, Gdańsk University of Technology have had multi-topical contacts both with the VWS and STG. Their representative, D.Sc.Eng. Edmund Brzoska took part in these events.

Faculty of Ocean Engineering and Ship Technology

Gdańsk University of Technology

New Missions And Visions Towards European Research Area

The Faculty of Ocean Engineering and Ship Technology of Technical University of Gdańsk has recently revised the objective of activities according to European Research Area assumptions. In this regard the new additional missions of Faculty are set:

- to enhance the productivity and effectiveness of the maritime sector of Poland as a member of EU
- to promote fast and efficient integration of Polish marine industry into EU and ERA (European Research Area)
- to provide the efficient structure for exchange of relevant knowledge and information within EU through organisation of international conferences, workshops and schools
- to promote a co-ordinated research effort in the maritime sector of the European Research Area, in particular to assist in creation of consortia participating in the European Framework Programmes
- to organise and support the short- and long-term exchange visits of researchers from and to EU
- to attract the promising young people into the research and production enterprises of the European maritime technology sector
- to organise and execute continuous training of highly qualified researchers through D.Sc. studies
- to organise and execute continuous training of designers in the most advanced and sophisticated design techniques through post-graduate courses
- to organise and execute continuous training of shipyard and co-operating industry staff in implementation of the advanced production techniques
- to organise and execute continuous training of the ship-owners and relevant state administration personnel in the problems of safe and reliable operation of the sea transport and offshore industry
- to provide expertise and highly qualified professional consultations to small and medium enterprises of the maritime sector of NAS (Newly Associated States).
- to create the efficient and well-organised structure for systematic collection, generation, exchange and dissemination of advanced and highly specialised knowledge between research organisations, educational institutions, shipyards and associated industries, ship-owners and state administration
- to initiate and continuously support a co-ordinated effort towards design, production and operation of durable, reliable, economic and technologically advanced ships.

Photo : Cezary Spigarski